Wsc1 acts as a piezosensor in *Saccharomyces cerevisiae*, enhancing glycerol efflux via aquaglyceroporin Fps1 in response to high hydrostatic pressure

Takahiro Mochizuki[*1], Toshiki Tanigawa[*1], Seiya Shindo[1], Momoka Suematsu[1], Yuki Oguchi[2], Tetsuo Mioka[1], Yusuke Kato[1], Mina Fujiyama[1], Eri Hatano[1], Masashi Yamaguchi[3], Hiroji Chibana[3], and Fumiyoshi Abe[1]†

[1]Department of Chemistry and Biological Science, College of Science and Engineering, Aoyama Gakuin University, [2]Center for Instrumental Analysis, College of Science and Engineering, Aoyama Gakuin University, 5-10-1 Fuchinobe, Chuo-ku, Sagamihara 252-5258, Japan; [3]Medical Mycology Research Center, Chiba University, 1-8-1 Inohana, Chuo-ku, Chiba 260-8673, Japan.

Running title: Wsc1 acts as a piezosensor in yeast.

Keywords: *Saccharomyces cerevisiae*, high hydrostatic pressure, hypoosmotic stress, CWI pathway, Wsc1, Fps1

Abbreviations: megapascals, MPa; cell wall integrity pathway, CWI pathway; calcofluor white, CFW

*These authors contributed equally.

†To whom correspondence should be addressed

Fumiyoshi Abe

Department of Chemistry and Biological Science, College of Science and Engineering, Aoyama Gakuin University, 5-10-1 Fuchinobe, Chuo-ku, Sagamihara 252-5258, Japan

Tel: +81-42-759-6233

E-mail: abef@chem.aoyama.ac.jp

Abstract

The fungal cell wall is the first barrier against diverse external stresses, such as high hydrostatic pressure. This study explores the roles of osmoregulation and the cell wall integrity (CWI) pathway in response to the high pressure in the yeast *Saccharomyces cerevisiae*. We demonstrate the roles of the transmembrane mechanosensor Wsc1 and aquaglyceroporin Fps1 in an underlying protective mechanism to avoid cellular rupture under high pressure. The promotion of water influx into cells at 25 MPa, as evident by an increase in cell volume and a loss of the plasma membrane eisosome structure, promotes the activation of Wsc1, an activator of the CWI pathway. The downstream mitogen-activated protein kinase Slt2 was hyperphosphorylated at 25 MPa. Glycerol efflux increases via Fps1 phosphorylation, which is initiated by downstream components of the CWI pathway, and contributes to the reduction in intracellular osmolarity under high pressure. Herein, the elucidation of a cellular pathway that is used as a protective mechanism against high pressure could potentially be translated to mammalian cells and could help to understand cellular mechanosensation and adaptation.

Introduction

Microorganisms encounter a wide variety of extreme environmental conditions, including heat, cold, pH, salinity, oxidants, or nutrient starvation. These stresses are first detected by sensor proteins that trigger the expression of specific genes via intracellular signaling pathways to respond to and overcome a crisis. Eukaryotes are also subjected to physical stresses, including tension, shear forces, and hydrostatic pressure. Mechanosensitive ion channels, found in eukaryotic cells, can directly sense various forms of mechanical forces, notably tension in the surrounding lipid bilayer (Kefauver et al., 2020, Ranade et al., 2015). In mammalian cells, forces are also detected, at the cell surface, through specific classes of integral membrane receptors, such as integrins and cadherins, which transduce stimuli into biochemical signals that initiate adaptive responses (Kechagia et al., 2019, Ladoux & Mege, 2017). Unlike stretching or expansion, hydrostatic pressure acts on cells as a uniform stress and affects all substances and reactions in the cell, according to Pascal's principle. Therefore, it is difficult to identify sensors of high hydrostatic pressure and determine the effects of this pressure on complex intracellular signaling networks. Nevertheless, there is ample evidence that cells modify their metabolism, transcription, translation, or post-translational modifications in response to increasing hydrostatic pressure (Abe et al., 1999, Abe, 2021, Bourges et al., 2017, Hodder et al., 2020, Iwahashi,

2015, Mishra et al., 2022, Pattappa et al., 2019).

Human cells also experience high hydrostatic pressures. In joints, cartilage is typically subjected to hydrostatic pressures between 3–10 MPa (0.1 MPa = 1 bar = 0.9869 atm = 1.0197 kg/cm^2) (Afoke et al., 1987), with a maximum pressure of 18 MPa in the hip joint (Hodge et al., 1989). In tissue engineering, hydrostatic pressures up to 50 MPa are used as a mechanical stimulus to induce chondrocyte differentiation (Elder & Athanasiou, 2009, Natenstedt et al., 2015). Furthermore, very low pressures, in the order of tens of mmHg, have recently received attention as a stimulus for endothelial tubulogenesis. The loading of endothelial cells with a pressure of 50 mmHg (~ 6.7 kPa) activates protein kinase C and transiently activates the Ras/ERK pathway as a result of the water efflux through aquaporin 1 (Yoshino et al., 2020). Microorganisms, such as *Escherichia coli* and *Saccharomyces cerevisiae,* also respond to hydrostatic pressure for growth and survival (Abe, 2007a, Abe, 2021, Aertsen et al., 2005, Marietou et al., 2015, Mota et al., 2013, Yoshino et al., 2020). High-pressure adaptation mechanisms in deep-sea microorganisms have also received considerable attention. However, little is known about how microbial cells detect such stimuli and convert them to intracellular signals.

Although *S. cerevisiae* is not a deep-sea piezophile, it can be used to elucidate the molecular mechanisms underlying the cell's responses to high hydrostatic pressure by applying basic knowledge of genetics and protein functions (Abe, 2021). Pressure pretreatment at a sublethal level (50 MPa for 1 h) increased the viability of yeast cells at 200 MPa, which is governed by two stress-induced transcription factors, Msn2 and Msn4 (Domitrovic et al., 2006). High pressure of 25 MPa generates superoxide anions in yeast mitochondria, and a strain deficient in superoxide dismutase 1 (Sod1) shows marked sensitivity to high pressures (Funada et al., 2022). Incubation of yeast cells at 25 MPa for 5 h resulted in the upregulation of the *DAN/TIR* family mannoprotein genes, which are known to be induced under hypoxic conditions and at low temperatures (Abe, 2007b). Target of rapamycin complex 1 (TORC1), an evolutionarily conserved serine/threonine kinase in eukaryotes, was activated by a pressure of 25 MPa (Uemura et al., 2020). We demonstrated that TORC1 plays a critical role in maintaining an appropriate glutamine level under high pressure by downregulating the *de novo* synthesis of glutamine (Uemura et al., 2020). Such evidence indicates that high-pressure stress induces diverse changes in intracellular processes and that cells survive by adaptively coping with each change.

87 The fungal cell wall provides the first barrier against external stresses, such as osmolarity
88 changes, harmful drugs, microbial enzymes, and mechanical injuries. It is an elastic structure with a
89 thickness of 50–500 nm and is composed of β1,3-glucan, β1,6-glucan, chitin, and mannoproteins
90 (Lesage & Bussey, 2006, Levin, 2011, Orlean, 2012). The Young's modulus of the cell wall is
91 estimated to be between 10 and 100 MPa (Davi et al., 2019, Ma et al., 2005), which is an intermediate
92 value between that of low-density polyethylene and rubber. The primary mechanical role of the cell
93 wall is to maintain cell morphology by balancing the tension generated by the turgor pressure, which
94 is important for polarized cell growth (Bi & Park, 2012, Madden & Snyder, 1998, Pruyne & Bretscher,
95 2000). During polarized growth, the cell wall is remodeled at the site of bud formation, by balancing
96 turgor pressure, to allow budding at the risk of cell lysis. In *S. cerevisiae,* cell wall destabilization is
97 sensed by transmembrane sensors of the WSC family (Wsc1, Wsc2, and Wsc3), as well as Mid2 and
98 its homolog Mtl1 (Jimenez-Gutierrez et al., 2020, Kock et al., 2015, Levin, 2005, Levin, 2011, Philip
99 & Levin, 2001), which activate a conserved signal transduction cascade, namely, the cell wall integrity
100 (CWI) pathway. These sensors have no sequence similarity but share a common structural feature
101 consisting of a large extracellular domain, transmembrane domain, and short cytoplasmic tail (Kock et
102 al., 2015, Rodicio & Heinisch, 2010). Their architecture is analogous to that of the mammalian
103 transmembrane integrins (Elhasi & Blomberg, 2019). Among the five sensor proteins in *S. cerevisiae*,
104 Wsc1 has been extensively studied both genetically and biophysically (Banavar et al., 2018, Dupres et
105 al., 2009, Heinisch et al., 2010, Merchan et al., 2004, Neeli-Venkata et al., 2021, Philip & Levin, 2001,
106 Schoppner et al., 2022). It is unevenly distributed at the cell surface and accumulates at sites of
107 polarized growth, in patches with an approximate diameter of 200 nm (Heinisch et al., 2010). Heat,
108 hypoosmotic shock, or treatment with cell wall-damaging agents and α-factor, all of which perturb the
109 cell wall, are sensed by Wsc1 to transiently activate the CWI pathway (Banavar et al., 2018, Cruz et
110 al., 2013, Kock et al., 2016, Straede & Heinisch, 2007). The extracellular domain of Wsc1 contains a
111 serine-threonine-rich (STR) region that is highly mannosylated (Lommel et al., 2004). Atomic force
112 microscopy (AFM) analysis showed that the STR domain has a nanospring-like structure that expands
113 and contracts under external pressure, which in turn causes dephosphorylation of the cytoplasmic tail
114 of Wsc1, transmitting signals downstream (Dupres et al., 2009, Heinisch et al., 2010, Vay et al., 2004).
115 The cytoplasmic tail of Wsc1 interacts with the GDP/GTP exchange factor Rom2, which subsequently
116 activates small GTPase Rho1(Philip & Levin, 2001, Vay et al., 2004). Bem2, Sac7, Lrg1, and Bag7 act

117 as GTPase-activating proteins (GAPs) for Rho1 (Fig. 1)(Martin et al., 2000, Peterson et al., 1994,
118 Schmidt et al., 1997, Schmidt et al., 2002). Rho1 regulates protein kinase C (Pkc1), a serine/threonine
119 protein kinase that is essential for cell wall remodeling (Levin, 2011). Pkc1 then activates three protein
120 kinase-signaling modules that integrate the mitogen-activated protein kinase kinase kinase
121 (MAPKKK) Bck1, redundant mitogen-activated protein kinase kinases (MAPKKs) Mkk1 and Mkk2,
122 and mitogen activated protein kinase (MAPK) Slt2 (Levin, 2011). Slt2 induces the transcription of
123 genes involved in maintaining cell wall integrity and mediates the phosphorylation of
124 aquaglyceroporin Fps1 (Ahmadpour et al., 2016, Levin, 2005, Mollapour et al., 2009). Although the
125 CWI cascade is well characterized (Fig. 1), the exact mode of Wsc1 action in response to different
126 environmental cues is still unclear.

127 Fps1 is under the control of the CWI pathway (Ahmadpour et al., 2016, Laz et al., 2020). In
128 yeast, when the cell wall is damaged, water flows into the cell driven by the osmotic pressure
129 difference between the inside and outside of the cell. To cope with this stress and prevent osmolysis,
130 yeast cells activate Fps1 to expel glycerol and eliminate osmotic pressure differences (Tamas et al.,
131 1999). The opening and closing of Fps1 is a complex process mediated by protein phosphorylation
132 involving several signaling pathways. First, MAP kinase Hog1 is activated in response to
133 hyperosmotic stress and phosphorylates the T231 residue of Fps1, resulting in Fps1 closure
134 (Ahmadpour et al., 2016). Hog1 negatively regulates this channel by displacing the Fps1-activating
135 proteins Rgc1 and Rgc2, thereby causing Fps1 closure (Lee et al., 2013). Second, it is known that the
136 open state of Fps1 requires phosphorylation by Ypk1, a target of TORC2-dependent protein kinase
137 (Muir et al., 2015). Third, Fps1 is known to promote opening by another MAP kinase, Slt2, which
138 phosphorylates the S537 residue of Fps1 (Muir et al., 2015).

139 To date, the effects of high hydrostatic pressure in yeast cells have not been studied with a
140 focus on osmoregulation and the CWI pathway. Remarkably, while imaging wild-type *S. cerevisiae*
141 cells, minor cell swelling was observed after high-pressure incubation at 25 MPa. This suggests that
142 high pressure may facilitate the influx of water into the cell or damage the cell wall allowing an influx
143 of water. This observation led us to study high-pressure signaling, with a focus on water influx, turgor
144 pressure, the CWI pathway via Wsc1, and aquaglyceroporin Fps1 (Fig. 1). We believe that our study
145 contributes important information on the signaling events triggered by the application of high-pressure
146 and the resulting molecular mechanisms that help the cell to cope with it.

147

148 **Results**

149 **Wsc1 is required for efficient cell growth under high pressure.**

150 The growth of any *S. cerevisiae* strain depends on tryptophan availability. Tryptophan-prototrophic
151 wild-type strains (e.g., BY4742) grew at 25 MPa with a doubling time of 5 h, whereas tryptophan
152 auxotrophic strains (e.g., YPH499) showed growth deficiency at this pressure (Abe & Horikoshi, 2000,
153 Abe & Minegishi, 2008). Therefore, BY4742 was used as a parental strain throughout the study. Based
154 on the previous studies (Jimenez-Gutierrez et al., 2020, Kock et al., 2015, Levin, 2005, Levin, 2011,
155 Philip & Levin, 2001), we hypothesized that any of the five sensor proteins, Wsc1–3, Mid2, and Mtl1,
156 could detect hydrostatic pressure changes, either directly or as a damage to the cell wall, and activate
157 the CWI pathway to allow for high-pressure growth. Cells were cultured in synthetic complete (SC)
158 medium at an OD_{600} of 0.01 for 48 h, under atmospheric pressure (0.1 MPa) or 25 MPa. Unless
159 otherwise specified, the high-pressure growth test was carried under these conditions throughout the
160 study. We found that the *wsc1*Δ mutant exhibited a moderate growth defect at 25 MPa, whereas the
161 other mutants grew as efficiently as the wild-type cells (Fig. 2A). The result suggests that Wsc1 plays
162 a primary role in high-pressure growth. To test the possibility that high pressure could impair the cell
163 wall, we examined the effect of the cell wall-stressing agent caspofungin, a β-glucan synthase
164 inhibitor (Kurtz & Douglas, 1997), on cell growth. We found that the drug inhibited cell growth more
165 effectively under high pressure than under atmospheric pressure, with an IC_{50} of 17.5 and 9.7 ng/mL at
166 0.1 and 25 MPa, respectively (Fig. 2B). These results suggest that high pressure additively impairs the
167 cell wall with caspofungin.

168 Wsc1 is characterized by an N-terminal extracellular cysteine-rich domain (CRD), followed
169 by a glycosylated STR domain, a single transmembrane domain, and a C-terminal cytoplasmic tail,
170 which is considered to be the mechanosensory region (Fig. 1). The CRD and STR domains detect
171 structural changes in the cell wall (Dupres et al., 2009, Heinisch et al., 2010). An alanine substitution
172 of eight cysteines in the CRD of Wsc1 had a marginal effect on high-pressure growth ability, whereas
173 deletions of the STR and the entire N-terminal region caused sensitivity to high pressure (Fig. 2C).
174 These results suggest that the STR of Wsc1 can detect structural changes in the cell wall caused by
175 high pressure.

176 Single-molecule AFM results indicated that Wsc1 assembles in patches as large as 200 nm

177 on the plasma membrane, thereby enhancing transduction of the CWI signaling pathway (Dupres et al.,
178 2009, Heinisch et al., 2010). Wsc1 assembles at the tips and bud necks where cells undergo polar
179 growth, and endocytosis is essential for their polarity (Piao et al., 2007). To determine the effect of
180 high pressure on the distribution of Wsc1, we observed the localization of Wsc1-GFP before and after
181 culturing the cells at 25 MPa. Cells were observed after depressurization. As previously reported (Piao
182 et al., 2007, Wilk et al., 2010), Wsc1-GFP localized mainly to bud tips, but also to the plasma
183 membrane of mother cells as patchy structures, and possibly to late endosomes as punctate structures
184 and vacuoles (Fig. 2D). High pressure enhanced vacuolar degradation of Wsc1, which was
185 characterized by increased vacuolar GFP signals, while maintaining the bud tip localization (Fig. 2D).
186 The polarized distribution of Wsc1 to bud tips requires endocytosis (Piao et al., 2007, Wilk et al.,
187 2010). The Wsc1 mutant, in which the NPF sequence at the C-terminal tail was replaced by AAA, and
188 a mutant strain lacking Sla1, a component of actin- and clathrin-based endocytic machinery, exhibited
189 a uniform distribution of Wsc1 within the plasma membrane (Piao et al., 2007). Although these
190 mutants are sensitive to caspofungin, they grow normally in its absence (Piao et al., 2007).
191 $Wsc1^{NPF>AAA}$-GFP was present throughout the plasma membrane (Fig. 2D) and $Wsc1^{NPF>AAA}$ -GFP
192 expressing cells grew as efficiently as the wild-type cells at 25 MPa (Fig. 2D). Therefore, we suggest
193 that Wsc1 is required for efficient cell growth under high pressure but does not need to be exclusively
194 localized to the bud tips.
195
196 **Wsc1 is a potential high-pressure sensor that transmits pressure signals to the CWI pathway.**
197 To address the role of Wsc1 as a high-pressure sensor, we focused on the downstream effector Rom2
198 during high-pressure growth. The Wsc1 C-terminal cytoplasmic domain residue, Y303, is critical for
199 its interaction with Rom2 (Vay et al., 2004). Both the disruption of *ROM2* and the Wsc1-Y303A
200 mutation, which interferes with the Wsc1–Rom2 interaction, resulted in growth defects at 25 MPa (Fig.
201 3A). Among the four Rho1 GAP genes, deletions in *BEM2, SAC7*, and *LRG1* caused growth defects at
202 25 MPa to varying degrees (Fig. 3A). The expression of GTP-bound active forms of Rho1-F35L or
203 Q68H failed to restore the high-pressure sensitivity of the *rom2*Δ mutant (Fig. 3B), suggesting that the
204 association of Rho1 with Rom2 is critically important for high-pressure growth. The expression of the
205 constitutively active form of Pkc1-R398P allowed the *rom2*Δ mutant to grow efficiently at 25 MPa
206 (Fig. 3B). Disruption of *PKC1*, *BCK1* or *SLT2* resulted in severe high-pressure sensitivity, whereas

207 only disruption of *MKK1* and not *MKK2* caused moderate high-pressure sensitivity (Fig. 3C).
208 Therefore, we suggest that Wsc1 acts as a piezosensor that detects hydrostatic pressure changes via
209 alteration of the cell wall structure and may convert pressure signals into the CWI pathway.

210 To further validate this hypothesis, the phosphorylation of Slt2 was examined in response to
211 high pressure. Remarkably, the phosphorylation of Slt2 increased in a pressure-dependent manner (Fig.
212 3D). Slt2 is under the control of the CWI signaling pathway, which is responsible for maintaining cell
213 wall homeostasis (Levin, 2005, Martin et al., 2000). Thus, hyperphosphorylated Slt2 may modulate
214 the transcription of downstream genes through phosphorylating its substrates under high pressures. To
215 test this possibility, we analyzed the effect of high pressure on the localization of Swi4, one of the
216 downstream transcription factors of Slt2. Wild-type cells that express Swi4-GFP were incubated with
217 15 μg/mL nocodazole in a YPD medium for 2 h at 0.1 MPa to induce cell cycle arrest in the G_2/M
218 phase (Kim et al., 2010) when most of the Swi4-GFP was present in the cytoplasm. Synthetic
219 Complete (SC) medium was not used in this analysis because nocodazole was ineffective in arresting
220 the cell cycle even at higher concentrations (our unpublished observation). Cells were then cultured
221 for 5 h at 0.1 MPa or 25 MPa. We found that the percentage of cells with Swi4-GFP migrating from
222 the cytoplasm to the nucleus was higher at 25 MPa (46%, n > 300) than at 0.1 MPa (17%, n > 300)
223 (Fig. 3E). Furthermore, cells lacking Swi4 or Swi6 showed marked high-pressure sensitivity (Fig. 3F).
224 These results support our model, which shows that high pressure activates the CWI pathway.
225

226 **High pressure facilitates water influx into the cells.**

227 While conducting this study, we noticed that the wild-type cells were moderately swollen after
228 incubation at 25 MPa. To validate this further, we examined whether the distribution of eisosomes was
229 affected by pressure. Eisosomes, peripheral membrane protein complexes located on the cytoplasmic
230 side of membrane compartments occupied by Can1 (MCC), are membrane invaginations composed of
231 furrows of approximately 50 nm in depth and 300 nm in length (Douglas & Konopka, 2014, Lanze et
232 al., 2020, Sakata et al., 2022). If the cell swells and the plasma membrane undergoes stretching under
233 high pressure, the membrane invaginations should disappear. To verify this, we observed cells
234 co-expressing the low-affinity tryptophan permease Tat1-GFP as a plasma membrane marker (Ishii et
235 al., 2022, Suzuki et al., 2013) and an eisosome resident protein, Nce102-mCherry, after cultured at 25
236 or 50 MPa. At 0.1 MPa, Nce102-mCherry was localized to the plasma membrane in a patchy pattern

237 characteristic of eisosomes (Fig. 4A). Notably, after high-pressure culture at 25 or 50 MPa,
238 Nce102-mCherry was evenly distributed within the plasma membrane (Fig. 4A). This was partially
239 suppressed by the presence of 1 M sorbitol (Fig. 4A). When the co-localization of Tat1-GFP and
240 Nce102-mCherry was examined at the cell surface, Pearson's correlation coefficient (PCC) increased
241 with incubation time at 25 MPa (Fig. 4B), confirming the even distribution of Nce102 under high
242 pressure. Similar increases in PCC with Tat1 were found for Pil1 and Sur7, another two
243 eisosome-associated proteins, but not as pronounced as for Nce102 (Fig. 4B). These results suggest
244 that the influx of water into the cells after high-pressure incubation results in tension in the plasma
245 membrane.

246 Therefore, we quantitatively analyzed the effect of high pressure on cell volume, which was
247 calculated by measuring the cell diameter using Tat1-GFP as the plasma membrane marker. We found
248 that the cell volume increased 1.2-fold after incubation at 25 MPa for 1 or 3 h, suggesting that water
249 influx occurred under high pressure (Fig. 4A, B). The degree of cell swelling was comparable even at
250 50 MPa, a pressure at which cell division stops. To verify pressure-induced cell swelling, we examined
251 the effects of 1 M sorbitol addition on cell volume under high pressure. As expected, 1 M sorbitol
252 suppressed the high pressure-induced increase in cell volume (Fig. 4B).

253 The yeast cell wall is composed of the mannoproteins, β1,3- and β1,6-glucan, and a small
254 amount of chitin, cross-linked to form elastic higher-order complexes (Lesage & Bussey, 2006).
255 Calcofluor white (CFW) is a chitin binding agent that causes cell wall injury. In the *cwh41*Δ mutant,
256 hypersensitivity to CFW is associated with cell wall abnormalities such as reduced levels of
257 β1,6-glucan (Ram et al., 1994). CFW inhibits the assembly of enzymes that connect chitin to
258 β1,3-glucan and β1,6-glucan. If high pressure causes cell wall injury, we hypothesized that sensitivity
259 to CFW may be enhanced. To validate this, we cultured cells at 0.1 or 25 MPa in the presence of
260 various concentrations of CFW in YPD medium. SC medium was not used in this analysis because
261 cells were substantially resistant to CFW in this medium (our unpublished observation). Although cell
262 growth was not inhibited at 0.1 MPa with 20 μg/mL CFW, it was significantly inhibited at 25 MPa
263 (Fig. 5A) at a lower concentration of 10 μg/mL CFW, suggesting that a high pressure enhances cell
264 sensitivity to CFW due to an increased accessibility of the drug to chitin. Although chitin was not
265 quantified in the cell wall after a high-pressure incubation, there was no noteworthy transcriptional
266 upregulation of the chitin synthetic genes at 25 MPa (Abe, 2007b). High-pressure enhanced CFW

267 susceptibility was a mild change compared to the effects observed upon *CWH41* gene disruption (Ram
268 et al., 1994). Thus, we assume that a high pressure of 25 MPa exerts a mild and possibly reversible
269 perturbation of cell wall integrity, resulting in an influx of water into the cell.

270 In growing yeast cells, turgor pressure is estimated to be 0.5–1.5 MPa due to the influx of
271 water driven by the osmotic gradient (Atilgan et al., 2015, Minc et al., 2014, Mishra et al., 2022,
272 Schaber et al., 2010). The turgor pushes the cell membrane, expanding the cell wall. Using an
273 osmometer, the osmotic pressure of the SC medium was found to be 255 ± 0 mOsm/kg (n = 3), which
274 corresponds to 0.588 MPa (nearly 0.6 MPa). Assuming that the turgor pressure of the cells was 1.0
275 MPa, the intracellular osmotic pressure was 1.6 MPa. Thus, the water potentials of the SC medium,
276 turgor pressure, and cells were –0.6, 1.0, and –1.6 MPa, respectively. Applying 1.0 MPa pressure to
277 the cell culture (i.e., the water potential of the SC medium will be 0.4 MPa) caused a water influx into
278 the cells until the turgor pressure rose to 2.0 MPa. Hence, the cell wall was subjected to twice the
279 turgor pressure even at 1.0 MPa compared to 0.1 MPa. This situation is similar to the exposure of cells
280 to hypoosmotic solutions. Even at external hydrostatic pressures above 1.0 MPa (e.g., 25 MPa), there
281 is no net water influx because there is no hydrostatic pressure difference between the inside and
282 outside of the cell, according to Pascal's principle. Thus, a turgor pressure of 2 MPa was maintained
283 throughout the incubation at 25 MPa. Eventually, the cell was at a higher risk of rupture under high
284 pressure. Furthermore, if the cell wall is physically injured by high pressure, the risk of rupture is
285 dramatically increased. To cope with this crisis, cells would prevent water influx by expelling glycerol,
286 the major osmolyte in yeast, to reduce internal osmotic pressure. Therefore, we focused on the
287 regulation of intracellular glycerol levels under high hydrostatic pressure.
288

289 **Aquaglyceroporin Fps1-mediated glycerol efflux is required for high-pressure growth.**

290 Under hyperosmotic conditions, yeast cells synthesize or retain high concentrations of glycerol to
291 maintain their osmotic balance (Blomberg, 2022, de Nadal & Posas, 2022, Hohmann, 2002).
292 Intracellular glycerol concentration is partially regulated by Fps1, an aquaglyceroporin on the plasma
293 membrane. Fps1 closes when extracellular osmolarity is high and opens when it is low, to expel
294 glycerol and prevent cell rupture (Ahmadpour et al., 2016, Beese et al., 2009, Lee et al., 2013, Luyten
295 et al., 1995, Muir et al., 2015). The growth of the *fps1*Δ mutant in SC medium was found to be
296 comparable to that of the wild-type strain at 0.1 MPa but was markedly sensitive at 25 MPa (Fig. 5B).

297 The addition of 1 M sorbitol to the medium restored the growth of the *fps1*Δ mutant to the wild-type
298 level, at 25 MPa (Fig. 5B). Disruption of the glycerol synthase genes *GPP1* or *GPD1* increased, albeit
299 partially, the high-pressure growth ability of the *fps1*Δ mutant (Fig. 5C). Furthermore, a single deletion
300 of *GPP1* enhanced high-pressure growth in the wild-type strain, although deletion of other glycerol
301 biosynthetic genes had no promotive effect (Fig. 5C).

302 Next, we analyzed the intracellular and extracellular glycerol concentrations. Wild-type and
303 *fps1*Δ cells in SC medium were incubated at 0.1 MPa and 25 MPa for 24 h, starting with an initial
304 OD_{600} of 0.1. Upon analyzing these cells, we found that the intracellular glycerol concentration in
305 wild-type cells decreased markedly after high-pressure culture, whereas more glycerol accumulated
306 extracellularly (Fig. 5D). By contrast, *fps1*Δ cells had a 3-fold higher intracellular glycerol
307 concentration than wild-type cells, which remained unchanged even after high-pressure culture (Fig.
308 5D). Thus, we concluded that wild-type cells expelled glycerol via Fps1 to cope with the high-pressure
309 induced excess water influx.

310 Furthermore, we observed the ultrastructure of cells by transmission electron microscopy
311 (TEM) and found that wild-type cells did not show any significant changes in cell morphology and the
312 cell wall structure after incubation at 25 MPa (Fig. 6). Interestingly, 20–40% of *fps1*Δ cells had
313 sharply ruptured cell walls, without any abnormalities in their intracellular structures at 25 MPa (Fig. 6,
314 arrows). It is likely that the cell walls were weakened by increased turgor pressure due to glycerol
315 accumulation under high pressure and were broken off during sample preparation using the sandwich
316 freezing method (Yamaguchi et al., 2021a, Yamaguchi et al., 2021b).

317

318 **Fps1 opening is likely regulated by Slt2 via phosphorylation during high-pressure cultures.**

319 The upstream regulators of Fps1 were analyzed to determine the mechanism by which cells regulate
320 Fps1 in response to high pressure. Previous studies have indicated that Hog1 is a negative regulator of
321 Fps1 opening, whereas Ypk1 and Slt2 are positive regulators (Fig. 1)(Ahmadpour et al., 2016, Lee et
322 al., 2013, Muir et al., 2015). To determine which kinases are involved in the regulation of the Fps1 in
323 response to high pressure, we examined the high-pressure growth ability of the *fps1*Δ mutant
324 expressing Fps1-T231A (Hog1 target site) or S537A (Slt2 target site) at 25 MPa. We found that the
325 Fps1-S537A strain showed high sensitivity, whereas the Fps1-T231A strain grew at 25 MPa as well as
326 the wild-type strain (Fig. 7A). We examined the phosphorylation of Fps1 using western blotting and

327 observed a high-molecular-weight band of Fps1-3HA, the intensity of which increased slightly (2.2 ±
328 0.3-fold, n = 3) with increasing pressure at 25 MPa (Fig. 7B). As expected, the high molecular weight
329 band of Fps1-3HA disappeared in cells expressing Fps1-S537A (Fig. 7B).

330 To clarify the importance of Slt2, we examined the effect of deletion of *SLT2* on
331 high-pressure growth and found that the *slt2*Δ mutant was highly sensitive to high pressure (Fig. 3C,
332 7C). Furthermore, this defect was completely rescued by the addition of 1M sorbitol (Fig. 7C). Thus,
333 the high-pressure sensitivity of the *slt2*Δ mutant was due to excess water influx, at least in part, due to
334 its inability to open Fps1 and expel glycerol. To verify whether the high-pressure sensitivity of the
335 *slt2*Δ mutant was due to reduced Fps1 activity, we introduced an *FPS1*-Δ11 plasmid into the *slt2*Δ
336 mutant. Fps1-Δ11 lacks amino acid residues 217–230, adjacent to the Hog1 phosphorylation site, T231,
337 essential for its closure. Thus, Fps1-Δ11 is constitutively active in expelling glycerol because of the
338 lack of Hog1-mediated channel closure (Tamas et al., 2003). We found that Fps1-Δ11 efficiently
339 rescued the high-pressure sensitivity of the *fps1*Δ mutant and partially rescued that of the *slt2*Δ mutant
340 (Fig. 7D).

341

342 **Ypk1 is required for growth under high pressure, independent of the regulation of Fps1.**

343 Fps1 is also phosphorylated by Ypk1 for its activation, depending on TORC2 signaling (Muir
344 et al., 2015). We found that the disruption of *YPK1* caused a severe defect in cell growth at 25 MPa,
345 demonstrating the importance of Ypk1. (Fig. 7E). Ypk1 is phosphorylated by multiple protein kinases
346 such as Fpk1/Fpk2 (Rispal et al., 2015), Pkh1/Pkh2 (Roelants et al., 2002, Roelants et al., 2004,
347 Roelants et al., 2010), and TORC2 (Leskoske et al., 2017, Muir et al., 2015, Roelants et al., 2004)(Fig.
348 1). To infer which kinases are required for high-pressure growth via phosphorylation of Ypk1, we
349 examined the effect of alanine substitutions for S51/S57 residues (Fpk1/Fpk2 target sites for Ypk1
350 inactivation), T504 residue (Pkh1/Pkh2 target site for Ypk1 activation), and S644/T662 residues
351 (TORC2 target sites for Ypk1 activation) on cell growth under high pressure (Fig. 1). While cells
352 expressing Ypk1-S51A-S71A grew as efficiently as wild-type cells at 25 MPa, those expressing
353 Ypk1-T504A or S644A-T662A showed severe growth defects under the pressure (Fig. 7E). Thus, it is
354 possible that Pkh1/Pkh2 and/or TORC2 phosphorylate Ypk1 in response to high pressure. As shown in
355 Fig. 4, cells swelled after high-pressure incubation and the eisosome structure disappeared. This raises
356 the possibility that Slm1, localized in the eisosome, is released by high pressure and eventually binds

357 to and activates TORC2, ultimately phosphorylating Ypk1 (Fig. 1)(Berchtold et al., 2012, Riggi et al.,
358 2018). To test this hypothesis in our preliminary experiments,
359 Lsp1-mCherry/Slm1-GFP-co-expressing and Avo3-3×mCherry/Slm1-GFP-co-expressing strains were
360 constructed, and any alterations in the colocalization of each strain under high pressure were observed
361 using confocal laser microscopy. Avo3 and Lsp1 are components of TORC2 and the eisosome,
362 respectively (Babst, 2019, Eltschinger & Loewith, 2016). We found that the colocalization of
363 Lsp1-mCherry and Slm1-GFP decreased after cell incubation at 25 MPa, whereas that of
364 Avo3-3×mCherry and Slm1-GFP appeared to increase, suggesting TORC2 activation (Fig. S1A).
365 Furthermore, phospho-Ypk1 was detected using a rabbit monoclonal antibody for phospho-PKC (pan)
366 (zeta Thr410) (190D10), which reacts with the phosphorylated T504 residue, and after incubation at
367 25 MPa for 3 h, its phosphorylation level increased 7-fold. (Fig. S1B).
368 To test whether phosphorylation of Fps1 by Ypk1 is required for high-pressure growth, the
369 effect of phosphorylation site mutations was examined. Residue S570 of Fps1 is majorly
370 phosphorylated by Ypk1, while the phosphorylation of residues S181 and S185 has also been reported
371 (Fig. 1, (Muir et al., 2015)). Both the Fps1-S570A-substituted and S181A-S185A-S570A
372 triple-substituted strains grew as well as the wild-type strain (Fig. 7F). Consistent with this result, the
373 electrophoretic mobility of the alanine substitution mutants Fps1-S570A-3HA,
374 Fps1-A181A-S185A-3HA, and Fps1-A181A-S185A-S570A-3HA remained unaffected (Fig. 7B).
375 Thus, Ypk1 is unlikely to phosphorylate Fps1 in response to high pressure.
376
377 **Discussion**
378 Based on the coincidental observation that cells swell moderately under high pressure, the importance
379 of glycerol efflux by Fps1 and its regulation via the CWI pathway became the focus of this study. We
380 propose the presence of a high-pressure signaling system mediated by the stress sensor Wsc1 (Fig. 8).
381 In our model, high hydrostatic pressure promoted water influx into yeast cells, resulting in increased
382 turgor pressure, which in turn expanded the cell walls and activated Wsc1. Since the *wsc1*Δ*mid2*Δ
383 double deletion mutant can only survive on osmotic support (Philip & Levin, 2001), Mid2 in particular
384 and the three other sensor proteins as well may have overlapping functions. It is interesting to note that
385 the water influx caused by the physical force of increased hydrostatic pressure was similar to that of
386 hypoosmotic stress. A high pressure of 25 MPa may also cause some perturbation to the cell wall, as

387 suggested by the observation that sensitivity of cells to CFW was enhanced under high pressure (Fig.
388 5A). This could be interpreted as the increased accessibility of CFW to chitin as a result of the
389 modification of cell wall. Since high hydrostatic pressure has little effect on covalent binding (Chen et
390 al., 2017), it is unlikely that the β1,3-glucan or β1,6-glucan networks are cleaved by high pressure.
391 Rather, we suspect that pressure may have a greater effect on the levels of cell wall mannoproteins.
392 Our previous DNA microarray results showed that transcription of genes encoding for the major cell
393 wall mannoprotein Cwp1 was markedly reduced under 25 MPa; instead, the *DAN/TIR* family
394 mannoprotein genes, which are typically induced under hypoxic conditions (Abramova et al., 2001),
395 were dramatically enhanced (Abe, 2007b). Although their protein levels have not been examined, the
396 composition of mannoproteins may change with high pressure, and eventually, cell wall elasticity may
397 change. It remains possible that high pressure directly causes a conformational change in Wsc1,
398 enhancing its interaction with Rom2. Once the CWI pathway is activated, Slt2 kinase phosphorylates
399 the aquaglyceroporin Fps1. Phosphorylation of Fps1 promotes its opening, allowing cells to expel
400 glycerol and adjust the osmotic pressure balance across the plasma membrane (Fig. 5). The *gpp1*Δ
401 mutant, which is partially defective in glycerol synthesis, grew slightly better at 25 MPa than the
402 wild-type strain. Therefore, a lower intracellular glycerol concentration may be advantageous for yeast
403 growth under high-pressure conditions. The role of Slt2 in growth under high pressure is not limited to
404 the activation of Fps1, but also the phosphorylation of Swi4/Swi6 and the induction of transcription of
405 many downstream genes. This seems justified by the fact that loss of *SWI4* or *SWI6* causes severe
406 high-pressure sensitivity (Fig. 3F).

407 However, there is a clear difference in the cellular responses to hypoosmotic stress and
408 pressure stress. For example, when cells that have been cultured in 1 M sorbitol medium are exposed
409 to hypoosmotic stress, by rapidly transferring them to a 0.1 M sorbitol medium, the response occurs
410 within 5 min, after which the phosphorylation level of Ypk1 and the activation levels of the HOG and
411 CWI pathways return to a steady state (Dunayevich et al., 2018, Muir et al., 2015, Riggi et al., 2018).
412 By contrast, in response to high hydrostatic pressure, the phosphorylation of Ypk1 does not change
413 within 5 min (unpublished observation), and phosphorylation of Ypk1 and Slt2 occurs after
414 approximately 3 h. Our high-pressure application was not as abrupt as an osmotic downshock and did
415 not modify the medium composition. Therefore, high-pressure application may be analogous to the
416 addition of low concentrations of cell wall synthesis inhibitors, such as caspofungin. Unlike cell wall

417 inhibitors, however, pressure does not introduce any substance into the system but simply affects the
418 interactions and equilibria between pre-existing components.

419 To answer the question of whether an increase in cell volume occurs during pressurization or
420 after depressurization, we introduced a high-pressure chamber with pressure-resistant optical windows
421 (Syn Cop., Kyoto, Japan) into an inverted microscope. Cells were placed on the optical window,
422 pressurized after the lid was tightened, and images were taken *in situ* during incubation at 25 MPa.
423 However, the variation in cell diameter during pressurization was so large that very small changes
424 could not be detected with any significant difference.

425 Our TEM observations suggest that the physical damage to the cell wall at 25 MPa was not
426 severe. If 24 h of incubation at 25 MPa caused significant damage to the cell wall, the cells should
427 rupture and die. However, this was not the case for either the wild-type strain or *fps1*Δ mutant.
428 Visualized in TEM images of *fps1*Δ cells, the cell wall ruptured sharply after a high-pressure
429 incubation (Fig. 6). This observation may be due to the localized weakening of the cell wall by
430 increased turgor pressure due to glycerol accumulation in the *fps1*Δ cells. Thus, they were likely
431 ruptured during TEM sample preparation by the sandwich freezing method (Yamaguchi et al., 2021a,
432 Yamaguchi et al., 2021b). However, the percentage of cell wall breaks in the *fps1*Δ strain after the
433 strain was incubated at 25 MPa varied by region on the copper disk, on which *fps1*Δ cells were placed,
434 as described in Materials and methods, and could not be quantitatively analyzed. In a pioneering study
435 by Perrier-Cornet et al., *S. fibuligera* cells were observed in a high-pressure optical chamber up to an
436 extreme pressure of 250 MPa, with a survival rate of 50% (Perrier-Cornet et al., 1995). They reported
437 a 10–15% reduction in cell volume after 10 min at 250 MPa and a 25% reduction in volume after
438 maintaining the pressure for another 15 min (Perrier-Cornet et al., 1995). An ultrahigh pressure of 250
439 MPa causes disruption of the membrane structure and protein denaturation; thus the intracellular
440 material leaks out of the cell, resulting in cell contraction (Perrier-Cornet et al., 1995). However, in our
441 study, we focused on cellular adaptation to mild pressure stress at 25 MPa, which permits cell growth.

442 A pertinent question is whether Wsc1 undergoes a direct conformational change, due to high
443 pressure, to transmit signals downstream, or whether the expansion of the cell wall, due to water influx,
444 activates Wsc1 indirectly, allowing for subsequent signaling. Using single-molecule AFM, Dupres et
445 al. demonstrated that Wsc1 behaves like a linear nanospring that is capable of resisting high
446 mechanical forces and responding to cell surface stress (Dupres et al., 2009). Recently, Neeli-Venkata

447 et al. reported the formation of large clusters of the surface protein Wsc1 at sites where forces were
448 applied to yeast cell walls (Neeli-Venkata et al., 2021). Wsc1 acts as a bona fide mechanosensor and
449 activates pathways that reinforce the cell wall (Neeli-Venkata et al., 2021). Owing to technical
450 difficulties in AFM of observing in a closed vessel under high pressure, it is currently not possible to
451 analyze pressure-induced structural changes in Wsc1 by AFM.

452 Although this study showed the importance of Ypk1 kinase in high-pressure growth (Fig. 7E),
453 it did not provide evidence that Ypk1 regulates the opening of Fps1 by phosphorylation (Fig. 7F).
454 Rather, alanine substitutions at Ypk1 residues, phosphorylated by TORC2 and Pkh1/Pkh2 kinases,
455 prevented high-pressure growth (Fig. 7E). TORC2-Ypk1 regulates polarization of the actin
456 cytoskeleton and sphingolipid biosynthesis (Kamada et al., 2005, Rispal et al., 2015, Roelants et al.,
457 2011, Tabuchi et al., 2006). Thus, the regulation of sphingolipid synthesis or actin organization may be
458 important for high-pressure adaptation. Indeed, high pressures stiffen membrane lipid bilayers
459 (Matsuki et al., 2013, Winter, 2002), which may adversely affect membrane protein functions,
460 membrane fusion, or membrane trafficking. Furthermore, hypoosmotic stress causes the
461 depolymerization of the actin cytoskeleton (Gualtieri et al., 2004). To cope with these pleiotropic
462 effects of high pressure, yeast cells may activate Fps1 via the CWI pathway to expel glycerol and
463 avoid cell rupture, promote sphingolipid synthesis via the TORC2-Ypk1 pathway to maintain
464 membrane homeostasis, and regulate actin cytoskeleton organization. Therefore, the regulation of
465 sphingolipid synthesis and actin cytoskeleton via the TORC2-Ypk1 pathway is an interesting research
466 target for understanding the physiological responses to high hydrostatic pressure in yeast.

467 Our previous studies have shown that defects in *TRP1*, *TAT2*, TORC1-EGOC, or poorly
468 characterized genes such as *EHG1/MAY24* cause severe high-pressure sensitivity (Abe & Horikoshi,
469 2000, Abe & Minegishi, 2008, Kurosaka et al., 2019, Uemura et al., 2020). On the contrary, the
470 defects in the CWI pathway and Fps1 shown in this study caused relatively mild sensitivity to
471 high-pressure. This is probably because the former defects cause impaired nutrient uptake or aberrant
472 glutamine accumulation under 25 MPa, resulting in rapid growth arrest after pressurization, whereas
473 the latter defects are due to an inability to prevent water influx under high pressure, which causes the
474 negative effects on growth to progress slowly. Yeasts possess two types of aquaporins, Aqy1 and Aqy2.
475 However, both alleles are nonfunctional in experimental strains derived from S288C, such as strain
476 BY4742 (Sabir et al., 2017). Therefore, the water influx into the cell when exposed to hypoosmotic or

477 high hydrostatic pressure stress is thought to be mainly due to passive diffusion across the plasma
478 membrane lipid bilayers. Passive diffusion of water across the lipid bilayer is much slower than water
479 flux through aquaporins. This could explain why the effects of high-pressure stress are relatively mild.
480 The Σ1278b strain and the naturally occurring *S. cerevisiae* strains have functional *AQY* alleles (Laize
481 et al., 1999). Therefore, the effects of hypoosmotic and high-pressure stress in these strains could be
482 more severe than in the experimental strains. The osmotic pressure of the SC medium was 255
483 mOsm/kg, which corresponds to 127.5 mM NaCl. When it rains, the ambient osmotic pressure drops
484 to near zero, exposing naturally occurring yeasts to greater hypoosmotic stress. Exposure to high
485 hydrostatic pressure under such low osmotic pressure would pose a threat to their survival.
486 Meanwhile, the ambient osmotic pressure is isotonic for human and other animal cells.
487 Therefore, excessive water influx due to high water pressure loading, as observed in yeast in this study,
488 would not occur. However, when human endothelial cells are subjected to a pressure of 50 mmHg
489 (~6.7 kPa), which corresponds to a transient increase in blood pressure during exercise, water is
490 extruded from the cell via aquaporin 1, causing cell contraction and plasma membrane deformation
491 (Yoshino et al., 2020). Consequently, protein kinase C is activated via the G protein-coupled receptor
492 and phospholipase C, which in turn activates the Ras/ERK pathway, ultimately leading to the
493 formation of complex tubular vascular structures (Yoshino et al., 2020). Since aquaporins are channels,
494 if the water potential is equivalent inside and outside the cells, no water efflux should occur even when
495 the pressure is 50 mmHg. However, because the pressure is very weak, the pressure applied at
496 different sites in a single cell may be different, and water may be extruded through aquaporins at
497 lower-pressure sites.
498
499 **Conclusion**
500 Hydrostatic pressure is a thermodynamic variable that merely affects the equilibrium or rate of
501 chemical reactions, without introducing any components into preexisting systems. One of the main
502 research targets of high-pressure bioscience and biotechnology is to reveal the mechanism by which
503 proteins form stable three-dimensional structures by analyzing the cavities and fluctuations inside the
504 molecules by spectroscopic and thermodynamic measurements under high pressure (Maeno &
505 Akasaka, 2015, Silva et al., 2006, Winter, 2019). On the other hand, in the food industry, ultra-high
506 pressures of several hundred MPa are used as an alternative to heating for sterilization of food

507 products and for food processing (Aganovic et al., 2021). In previous studies, experiments were
508 carried out under equilibrium conditions. Therefore, the results were observed a sufficiently long time
509 after pressurization. However, our study aimed to elucidate the molecular mechanisms by which living
510 cells recognize mild "high pressures" of a few tens of MPa and how they adapt to the new
511 environments by modifying their complex intracellular metabolism and gene expression. Pressure
512 affects all molecules and cellular reactions according to Pascal's principle, but the effects vary not only
513 with the magnitude of the applied pressure but also with the duration of the pressurization. Therefore,
514 the effects of high pressure on the complex metabolic processes of living cell systems cannot be
515 generalized. We believe that the full picture of pressure effects will be revealed by applying the
516 extensive knowledge of yeast cell biology and sophisticated molecular genetic tools to advanced
517 transcriptomics, proteomics, and metabolomics studies, which could potentially be translated to
518 mammalian cells and help improve cellular health under normal and stress conditions.
519

520 **Materials and methods**

521 **Yeast strains and media**

522 The parental wild-type strain BY4742 and deletion mutants were used in this study (Table 1). Strains
523 DL376 (*pkc1*Δ) and DL100 (the parental strain of DL376) were kindly provided by Dr. David Levin of
524 Boston University Goldman School of Dental Medicine through Dr. Hidetoshi Iida of Tokyo Gakugei
525 University (Levin & Bartlett-Heubusch, 1992). The two strains were transformed with YCplac22
526 (*TRP1, CEN*) to provide tryptophan prototrophy. Cells were grown in SC medium or YPD medium at
527 25 °C under 0.1 MPa or 25 MPa (Abe & Minegishi, 2008). The SC medium contained 0.67% yeast
528 nitrogen base without amino acids (Becton, Dickinson and Company, MD, USA), 2% D-glucose, 20
529 μg/mL methionine, 90 μg/mL leucine, 30 μg/mL isoleucine, 40 μg/mL tryptophan, 20 μg/mL histidine,
530 30 μg/mL lysine, 20 μg/mL methionine, 50 μg/mL phenylalanine, 30 μg/mL tyrosine, 20 μg/mL
531 arginine, 100 μg/mL aspartic acid, 100 μg/mL glutamic acid, 400 μg/mL serine, and 200 μg/mL
532 threonine. YPD medium contains 1% Bacto yeast extract (Becton, Dickinson and Company), 2%
533 Bacto peptone (Becton, Dickinson and Company), and 2% D-glucose.
534

535 **High-pressure cell culture**

536 For most experiments examining growth efficiency under high pressure, growing cells in shaking

537 culture were diluted in SC or YPD medium to an OD_{600} of 0.01. The diluted cells were transferred to
538 sterile 2.2-mL tubes and sealed with Parafilm™ (Bemis Corp., Neenah, WI, USA). The tubes were
539 placed in a 500-mL high-pressure chamber (Abe & Minegishi, 2008) and subjected to 25 MPa at
540 25 °C for 48 h. After depressurization, cell growth was evaluated by measuring OD_{600} using a PD-303
541 spectrophotometer (Apel, Kawaguchi, Japan). Here, OD_{600} = 1.0 corresponds to 1.65×10^7 cells/mL in
542 our device setup.
543
544 **Generation of plasmids and mutant strains**
545 The plasmids used in the present study are listed in Table 2. Polymerase chain reaction (PCR)-based
546 site-directed mutagenesis was performed using the appropriate primers. The primer sequences will be
547 disclosed upon request. Homologous recombination, using pJT6 (GFP, *HIS3*) and pJT601 (mCherry,
548 *URA3*), was used to tag genes in the yeast genome with GFP and mCherry, respectively (kind gifts
549 from Dr. Jiro Toshima of Tokyo University of Science, (Kawada et al., 2015)). Plasmids encoding
550 HA-Rho1 (SP333; *LEU2, CEN*), HA-Rho1^{F35L} (SP335; *LEU2, CEN*), and HA-Rho1^{Q68H} (SP336;
551 *LEU2, CEN*) were kindly provided by Dr. Satoshi Yoshida of Waseda University (19339687).
552 pBSK-*SFK1*-3×mCherry-*CaURA3* was kindly provided by Dr. Takuma Kishimoto of Hokkaido
553 University Graduate School of Life Science (Kishimoto et al., 2021). To generate Avo3-3×mCherry
554 strain, a DNA fragment encoding a *C*-terminal domain of Avo3 was amplified by PCR and was
555 inserted into pBSK-*SFK1*-3×mCherry-*CaURA3* of which *SFK1* gene had been removed. The resulting
556 plasmid was linearized by digestion with *Eco*RV and introduced into the wild-type strain harboring
557 *SLM1*-GFP in the genome.
558
559 **Western blotting**
560 Whole-cell extract preparation was performed as previously described (Ishii et al., 2022). Briefly, 1.65
561 $\times 10^8$ cells were collected by centrifugation, serially washed with 10 mM NaN_3, 10 mM NaF and lysis
562 buffer A (50 mM Tris-HCl, 5 mM EDTA, 10 mM NaN_3, and Complete™ EDTA-free tablet; Roche
563 Diagnostics, Mannheim, Germany), and disrupted with glass beads at 4 °C. Unbroken cells and debris
564 were removed by centrifugation at 900 × *g* for 5 min, and purified lysates were treated with 5% (w/v)
565 Sodium dodecyl sulfate (SDS) and 5% (v/v) 2-mercaptoethanol at 37 °C for 10 min. Whole-cell
566 extract preparation to detect phospho-Slt2 was performed as previously described (Wilk et al., 2010)

567 with some modifications. Yeast cells amounting to 5×10^7 in SC medium were treated with 255 mM
568 NaOH–1% 2-mercaptoethanol on ice for 15 min, then 6% trichloroacetic acid (TCA) was added and
569 cells were kept on ice for another 15 min. The cell pellet was collected after centrifugation at 15,000 ×
570 *g* for 5 min, washed with 1 M Tris-HCl (pH 6.8), and was treated with a sample buffer (65 mM Tris
571 [pH6.8], 2% SDS, 10% Glycerol, 100 mM DTT, 0.002% BPB) to denature proteins at 95 °C for 5 min.
572 The supernatant after centrifugation at 15,000 × *g* for 5 min was used for western blotting. Whole-cell
573 extract preparation to detect phospho-Ypk1was performed as previously described (Roelants et al.,
574 2011) with some modifications. Yeast cells amounting to 1.65×10^7 were collected by centrifugation
575 at 6,000 × *g* for 1 min. After removing the supernatant, the cell pellet was frozen in liquid nitrogen and
576 was treated with 150 μL of 1.85 M NaOH–7.4% 2-mercaptoethanol for 15 min on ice. Then, 150 μL
577 of 50% TCA was added to the cell suspension to precipitate proteins on ice for 10 min. After removing
578 the supernatant, the proteins were washed twice with acetone and were denatured with the sample
579 buffer at 95 °C for 5 min. Proteins were separated by SDS-PAGE and transferred to Immobilon PVDF
580 membranes (EMD Millipore, Billerica, MA, USA). The membrane was incubated for 1 h with
581 antibodies. The following antibodies were used: a monoclonal antibody for HA (Medical & Biological
582 Laboratories Co. Ltd., Nagoya, Japan), a rabbit polyclonal antibody for Adh1 (Rockland
583 Immunochemicals, Inc., Gilbersville, PA, USA), a rabbit polyclonal antibody for Pma1 (Usami et al.,
584 2014), a mouse monoclonal antibody for Slt2 (cat. no. sc-133189, Santa Cruz Biotechnology, TX,
585 USA), a rabbit monoclonal antibody phospho-p44/42 MAPK (Erk1/2, Thr202/Tyr204; cat no. 4376,
586 Cell Signaling Technology, MA, USA) to detect phospho-Slt2, a rabbit polyclonal antibody for Ypk1
587 (a kind gift from Dr. Mitsuaki Tabuchi of Kagawa University), and a rabbit monoclonal antibody for
588 Phospho-PKC (pan) (zeta Thr410) (190D10) (cat. no. 2060, Signaling Technology) to detect
589 phospho-Ypk1. The membranes were washed and incubated for 30 min with horseradish
590 peroxidase-conjugated goat anti-rabbit IgG (GE Healthcare Bio-Sciences, NJ, USA). Labeling was
591 performed using an enhanced chemiluminescence (ECL) select kit (GE Healthcare Bio-Sciences). The
592 chemiluminescence signals were detected in an ImageQuant LAS4000 mini (GE Healthcare Life
593 Sciences, NJ, USA)
594
595 **Image collection and analyses on confocal laser microscope**
596 Cells expressing GFP- or mCherry-tagged proteins were imaged using a confocal laser microscope

597 (FV-3000) equipped with an objective lens UPLAPO60XOHR (NA 1.5) (Olympus, Co. Ltd., Tokyo,
598 Japan). To determine the cell volume, cells were assumed to be spheres or ellipsoids. Using Tat1-GFP
599 as a cell membrane marker (Ishii et al., 2022), cross-sectional images of > 100 cells cultured under
600 each condition were acquired. CellSens software (Olympus, Co. Ltd) was used to mark Tat1-GFP as a
601 circle or ellipse, and the radius (r μm) or long (a μm) and short radii (b μm) were calculated. For
602 spheres, the volume (μm^3) was approximated by $V = 4/3\pi * r^3$, and for ellipsoids, $V = 4/3\pi * a * b^2$.
603 Changes in cell volume due to high-pressure incubation were measured by acquiring images at 0.1
604 MPa, immediately after depressurization. Colocalization of Lsp1-mCherry with Slm1-GFP or
605 Avo3-3×mCherry with Slm1-GFP was analyzed in more than 50 cells from three independent
606 experiments using cellSens software and represented by the Pearson colocalization coefficient. An
607 IX70 epifluorescence inverted microscope (Olympus, Co. Ltd.) was used for imaging.
608
609 **Determination of glycerol concentration**
610 Culture medium containing cells of 1.0 OD_{600} (1.65×10^7 cells) was centrifuged at 6,000 × g for 1 min
611 to separate the supernatant and cell pellet. The cell pellet was dissolved in 100 μL of sterilized
612 deionized water and the mixture was heated at 95 °C for 10 min. After cooling, the mixture was
613 centrifuged at 21,500 × g for 10 min to collect the supernatant. Glycerol concentrations in the samples
614 were determined using a glycerol colorimetric assay kit (item no. 10010755, Cayman Chemical
615 Company, MI, USA) with an appropriate dilution.
616
617 **Measurement of osmotic pressure**
618 The osmotic pressure of SC medium was measured using a Fiske 210 osmometer (Advanced
619 Instruments, MA, USA).
620
621 **Transmission electron microscopy observation**
622 Samples for TEM observation were prepared as described previously (Yamaguchi et al., 2021a,
623 Yamaguchi et al., 2021b), with modifications. Cells cultured at 0.1 MPa or 25 MPa for 24 h in the SC
624 medium were briefly centrifuged at 760 × g following depressurization, and less than 1 μL of the cell
625 suspension was sandwiched between two copper disks (3 mm diameter) that had been
626 prehydrophilized. The copper disks were then sandwiched between reverse-acting tweezers and

627 dropped into a coolant for quick freezing. An isopentane : ethanol (4:1) mixture cooled with liquid
628 nitrogen to a sherbet-like consistency (approximately –130 °C) was used as the coolant. The copper
629 disks were immediately transferred to liquid nitrogen, cracked open, and then transferred to a fixing
630 solution cooled with liquid nitrogen. Ethanol containing 2% glutaraldehyde and 1% tannic acid was
631 used as a fixing solution. The samples in the fixing solution were kept at –80 °C for 48 h, –20 °C for 2
632 h, 4 °C for 2 h, and finally returned to room temperature, in that order. Cells on copper disks were
633 immersed in dehydrated ethanol for 30 min thrice and then overnight. Propylene oxide : resin (Agar
634 low viscosity resin LV, cat. no. R1078, Agar Scientific Ltd, Essex, UK) mixture was used for resin
635 replacement of the samples, with the following mixing ratios in sequence; 1 : 0 (30 min, twice), 2 : 1
636 (1 h, once), 1 : 2 (1 h, once), 0 : 1 (overnight, once). The resin-substituted samples were allowed to
637 solidify for 24 h at 60 °C. Ultrathin sections of 70 nm thickness were then prepared using an Ultracut
638 E ultramicrotome (Reichert-Jung, Austria). The sections were stained with EM Stainer (cat no. 336,
639 Nissin EM, Tokyo, Japan) for 30 min and lead stain (Sigma-Aldrich, MO, USA) for 30 min. The
640 samples were observed using a transmission electron microscope JEM-2100 (JEOL, Tokyo, Japan)
641 equipped with a thermionic electron emission electron gun (LaB6 filament) at an acceleration voltage
642 of 100 kV.
643
644 **Acknowledgements**
645 We would like to thank Drs. Satoshi Yoshida, Jiro Toshima, Makoto Nagano, Takuma Kishimoto for
646 providing plasmids; Drs. David Levin and Hidetoshi Iida for providing yeast strains; Dr. Mitsuaki
647 Tabuchi for providing an antibody and critical reading of this manuscript; Mrs. Katsuyuki Uematsu
648 and Yosuke Ishihara for technical assistances on TEM sample preparations; the laboratory members
649 for facilitating valuable discussions. TEM observation was supported by Center for Instrumental
650 Analysis, College of Science and Engineering, Aoyama Gakuin University.
651
652 **Funding**
653 This work was supported by a grant from the Japan Society for the Promotion of Science (No.
654 18K05397 and 22H02247 to F. Abe), and a fund from Aoyama Gakuin University (Aoyama Vision
655 2019–2021).
656

657 **Author contributions**

658 Takahiro Mochizuki: Conceptualization and investigation, Toshiki Tanigawa: Conceptualization and
659 investigation, Seiya Shindo: Investigation, Momoka Suematsu: Investigation, Yuki Oguchi:
660 Investigation, Tetsuo Mioka: Cooperation, Yusuke Kato: Cooperation, Mina Fujiyama: Investigation,
661 Eri Hatano: Investigation, Masashi Yamaguchi: Cooperation, Hiroji Chibana: Cooperation, Fumiyoshi
662 Abe: Conceptualization; supervision; writing – original draft, review and editing.

663

664 **Competing interests**

665 The authors declare no competing interests.

666

667 **References**

668 Abe F (2021) Molecular responses to high hydrostatic pressure in eukaryotes: Genetic insights from
669 studies on *Saccharomyces cerevisiae*. *Biology (Basel)* **10**: 10.3390/biology10121305

670 Abe F (2007a) Exploration of the effects of high hydrostatic pressure on microbial growth, physiology
671 and survival: perspectives from piezophysiology. *Biosci Biotechnol Biochem* **71**: 2347-2357

672 Abe F (2007b) Induction of *DAN/TIR* yeast cell wall mannoprotein genes in response to high
673 hydrostatic pressure and low temperature. *FEBS Lett* **581**: 4993-4998

674 Abe F & Horikoshi K (2000) Tryptophan permease gene *TAT2* confers high-pressure growth in
675 *Saccharomyces cerevisiae*. *Mol Cell Biol* **20**: 8093-8102

676 Abe F, Kato C, & Horikoshi K (1999) Pressure-regulated metabolism in microorganisms. *Trends*
677 *Microbiol* **7**: 447-453

678 Abe F & Minegishi H (2008) Global screening of genes essential for growth in high-pressure and cold
679 environments: searching for basic adaptive strategies using a yeast deletion library. *Genetics* **178**:
680 851-872

681 Abramova NE, Cohen BD, Sertil O, Kapoor R, Davies KJ, & Lowry CV (2001) Regulatory
682 mechanisms controlling expression of the *DAN/TIR* mannoprotein genes during anaerobic
683 remodeling of the cell wall in *Saccharomyces cerevisiae*. *Genetics* **157**: 1169-1177

684 Aertsen A, De Spiegeleer P, Vanoirbeek K, Lavilla M, & Michiels CW (2005) Induction of oxidative
685 stress by high hydrostatic pressure in Escherichia coli. *Appl Environ Microbiol* **71**: 2226-2231

686 Afoke NY, Byers PD, & Hutton WC (1987) Contact pressures in the human hip joint. *J Bone Joint*

687 *Surg Br* **69**: 536-541
688 Aganovic K, Hertel C, Vogel RF, Johne R, Schluter O, Schwarzenbolz U, Jager H, Holzhauser T,
689 Bergmair J, Roth A, Sevenich R, Bandick N, Kulling SE, Knorr D, Engel KH, & Heinz V (2021)
690 Aspects of high hydrostatic pressure food processing: Perspectives on technology and food safety.
691 *Compr Rev Food Sci Food Saf* **20**: 3225-3266
692 Ahmadpour D, Maciaszczyk-Dziubinska E, Babazadeh R, Dahal S, Migocka M, Andersson M,
693 Wysocki R, Tamas MJ, & Hohmann S (2016) The mitogen-activated protein kinase Slt2
694 modulates arsenite transport through the aquaglyceroporin Fps1. *FEBS Lett* **590**: 3649-3659
695 Atilgan E, Magidson V, Khodjakov A, & Chang F (2015) Morphogenesis of the Fission Yeast Cell
696 through Cell Wall Expansion. *Curr Biol* **25**: 2150-2157
697 Babst M (2019) Eisosomes at the intersection of TORC1 and TORC2 regulation. *Traffic* **20**: 543-551
698 Banavar SP, Gomez C, Trogdon M, Petzold LR, Yi TM, & Campas O (2018) Mechanical feedback
699 coordinates cell wall expansion and assembly in yeast mating morphogenesis. *PLoS Comput Biol*
700 **14**: e1005940
701 Beese SE, Negishi T, & Levin DE (2009) Identification of positive regulators of the yeast fps1
702 glycerol channel. *PLoS Genet* **5**: e1000738
703 Berchtold D, Piccolis M, Chiaruttini N, Riezman I, Riezman H, Roux A, Walther TC, & Loewith R
704 (2012) Plasma membrane stress induces relocalization of Slm proteins and activation of TORC2
705 to promote sphingolipid synthesis. *Nat Cell Biol* **14**: 542-547
706 Bi E & Park HO (2012) Cell polarization and cytokinesis in budding yeast. *Genetics* **191**: 347-387
707 Blomberg A (2022) Yeast osmoregulation - glycerol still in pole position. *FEMS Yeast Res* **22**:
708 10.1093/femsyr/foac035
709 Bourges AC, Torres Montaguth OE, Ghosh A, Tadesse WM, Declerck N, Aertsen A, & Royer CA
710 (2017) High pressure activation of the Mrr restriction endonuclease in *Escherichia coli* involves
711 tetramer dissociation. *Nucleic Acids Res* **45**: 5323-5332
712 Brachmann CB, Davies A, Cost GJ, Caputo E, Li J, Hieter P, & Boeke JD (1998) Designer deletion
713 strains derived from *Saccharomyces cerevisiae* S288C: a useful set of strains and plasmids for
714 PCR-mediated gene disruption and other applications. *Yeast* **14**: 115-132
715 Chen B, Hoffmann R, & Cammi R (2017) The effect of pressure on organic reactions in fluids-a new
716 theoretical perspective. *Angew Chem Int Ed Engl* **56**: 11126-11142

717 Cruz S, Munoz S, Manjon E, Garcia P, & Sanchez Y (2013) The fission yeast cell wall stress
718 sensor-like proteins Mtl2 and Wsc1 act by turning on the GTPase Rho1p but act independently of
719 the cell wall integrity pathway. *Microbiologyopen* **2**: 778-794
720 Davi V, Chevalier L, Guo H, Tanimoto H, Barrett K, Couturier E, Boudaoud A, & Minc N (2019)
721 Systematic mapping of cell wall mechanics in the regulation of cell morphogenesis. *Proc Natl*
722 *Acad Sci U S A* **116**: 13833-13838
723 de Nadal E & Posas F (2022) The HOG pathway and the regulation of osmoadaptive responses in
724 yeast. *FEMS Yeast Res* **22**: 10.1093/femsyr/foac013
725 Domitrovic T, Fernandes CM, Boy-Marcotte E, & Kurtenbach E (2006) High hydrostatic pressure
726 activates gene expression through Msn2/4 stress transcription factors which are involved in the
727 acquired tolerance by mild pressure precondition in *Saccharomyces cerevisiae*. *FEBS Lett* **580**:
728 6033-6038
729 Douglas LM & Konopka JB (2014) Fungal membrane organization: the eisosome concept. *Annu Rev*
730 *Microbiol* **68**: 377-393
731 Dunayevich P, Baltanas R, Clemente JA, Couto A, Sapochnik D, Vasen G, & Colman-Lerner A (2018)
732 Heat-stress triggers MAPK crosstalk to turn on the hyperosmotic response pathway. *Sci Rep* **8**:
733 15168-018-33203-6
734 Dupres V, Alsteens D, Wilk S, Hansen B, Heinisch JJ, & Dufrene YF (2009) The yeast Wsc1 cell
735 surface sensor behaves like a nanospring in vivo. *Nat Chem Biol* **5**: 857-862
736 Elder BD & Athanasiou KA (2009) Hydrostatic pressure in articular cartilage tissue engineering: from
737 chondrocytes to tissue regeneration. *Tissue Eng Part B Rev* **15**: 43-53
738 Elhasi T & Blomberg A (2019) Integrins in disguise - mechanosensors in *Saccharomyces cerevisiae* as
739 functional integrin analogues. *Microb Cell* **6**: 335-355
740 Eltschinger S & Loewith R (2016) TOR Complexes and the Maintenance of Cellular Homeostasis.
741 *Trends Cell Biol* **26**: 148-159
742 Funada C, Tanino N, Fukaya M, Mikajiri Y, Nishiguchi M, Otake M, Nakasuji H, Kawahito R, & Abe
743 F (2022) *SOD1* mutations cause hypersensitivity to high-pressure-induced oxidative stress in
744 *Saccharomyces cerevisiae*. *Biochim Biophys Acta Gen Subj* **1866**: 130049
745 Gietz RD & Sugino A (1988) New yeast-Escherichia coli shuttle vectors constructed with in vitro
746 mutagenized yeast genes lacking six-base pair restriction sites. *Gene* **74**: 527-534

747 Gualtieri T, Ragni E, Mizzi L, Fascio U, & Popolo L (2004) The cell wall sensor Wsc1p is involved in
748 reorganization of actin cytoskeleton in response to hypo-osmotic shock in *Saccharomyces*
749 *cerevisiae*. *Yeast* **21**: 1107-1120
750 Heinisch JJ, Dupres V, Wilk S, Jendretzki A, & Dufrene YF (2010) Single-molecule atomic force
751 microscopy reveals clustering of the yeast plasma-membrane sensor Wsc1. *PLoS One* **5**: e11104
752 Hodder E, Guppy F, Covill D, & Bush P (2020) The effect of hydrostatic pressure on proteoglycan
753 production in articular cartilage in vitro: a meta-analysis. *Osteoarthritis Cartilage* **28**: 1007-1019
754 Hodge WA, Carlson KL, Fijan RS, Burgess RG, Riley PO, Harris WH, & Mann RW (1989) Contact
755 pressures from an instrumented hip endoprosthesis. *J Bone Joint Surg Am* **71**: 1378-1386
756 Hohmann S (2002) Osmotic stress signaling and osmoadaptation in yeasts. *Microbiol Mol Biol Rev*
757 **66**: 300-372
758 Ishii R, Fukui A, Sakihama Y, Kitsukawa S, Futami A, Mochizuki T, Nagano M, Toshima J, & Abe F
759 (2022) Substrate-induced differential degradation and partitioning of the two tryptophan
760 permeases Tat1 and Tat2 into eisosomes in *Saccharomyces cerevisiae*. *Biochim Biophys Acta*
761 *Biomembr* **1864**: 183858
762 Iwahashi H (2015) Pressure-Dependent Gene Activation in Yeast Cells. *Subcell Biochem* **72**: 407-422
763 Jimenez-Gutierrez E, Alegria-Carrasco E, Sellers-Moya A, Molina M, & Martin H (2020) Not just the
764 wall: the other ways to turn the yeast CWI pathway on. *Int Microbiol* **23**: 107-119
765 Kamada Y, Fujioka Y, Suzuki NN, Inagaki F, Wullschleger S, Loewith R, Hall MN, & Ohsumi Y
766 (2005) Tor2 directly phosphorylates the AGC kinase Ypk2 to regulate actin polarization. *Mol Cell*
767 *Biol* **25**: 7239-7248
768 Kawada D, Kobayashi H, Tomita T, Nakata E, Nagano M, Siekhaus DE, Toshima JY, & Toshima J
769 (2015) The yeast Arf-GAP Glo3p is required for the endocytic recycling of cell surface proteins.
770 *Biochim Biophys Acta* **1853**: 144-156
771 Kechagia JZ, Ivaska J, & Roca-Cusachs P (2019) Integrins as biomechanical sensors of the
772 microenvironment. *Nat Rev Mol Cell Biol* **20**: 457-473
773 Kefauver JM, Ward AB, & Patapoutian A (2020) Discoveries in structure and physiology of
774 mechanically activated ion channels. *Nature* **587**: 567-576
775 Kim KY, Truman AW, Caesar S, Schlenstedt G, & Levin DE (2010) Yeast Mpk1 cell wall integrity
776 mitogen-activated protein kinase regulates nucleocytoplasmic shuttling of the Swi6

777 transcriptional regulator. *Mol Biol Cell* **21**: 1609-1619
778 Kishimoto T, Mioka T, Itoh E, Williams DE, Andersen RJ, & Tanaka K (2021) Phospholipid flippases
779 and Sfk1 are essential for the retention of ergosterol in the plasma membrane. *Mol Biol Cell* **32**:
780 1374-1392
781 Kock C, Arlt H, Ungermann C, & Heinisch JJ (2016) Yeast cell wall integrity sensors form specific
782 plasma membrane microdomains important for signalling. *Cell Microbiol* **18**: 1251-1267
783 Kock C, Dufrene YF, & Heinisch JJ (2015) Up against the wall: is yeast cell wall integrity ensured by
784 mechanosensing in plasma membrane microdomains? *Appl Environ Microbiol* **81**: 806-811
785 Kurosaka G, Uemura S, Mochizuki T, Kozaki Y, Hozumi A, Suwa S, Ishii R, Kato Y, Imura S, Ishida
786 N, Noda Y, & Abe F (2019) A novel ER membrane protein Ehg1/May24 plays a critical role in
787 maintaining multiple nutrient permeases in yeast under high-pressure perturbation. *Sci Rep* **9**:
788 18341-019-54925-1
789 Kurtz MB & Douglas CM (1997) Lipopeptide inhibitors of fungal glucan synthase. *J Med Vet Mycol*
790 **35**: 79-86
791 Ladoux B & Mege RM (2017) Mechanobiology of collective cell behaviors. *Nat Rev Mol Cell Biol*
792 **18**: 743-757
793 Laize V, Gobin R, Rousselet G, Badier C, Hohmann S, Ripoche P, & Tacnet F (1999) Molecular and
794 functional study of *AQY1* from *Saccharomyces cerevisiae*: role of the C-terminal domain.
795 *Biochem Biophys Res Commun* **257**: 139-144
796 Lanze CE, Gandra RM, Foderaro JE, Swenson KA, Douglas LM, & Konopka JB (2020) Plasma
797 Membrane MCC/Eisosome Domains Promote Stress Resistance in Fungi. *Microbiol Mol Biol Rev*
798 **84**: 10.1128/MMBR.00063-19. Print 2020 Nov 18
799 Laz EV, Lee J, & Levin DE (2020) Crosstalk between *Saccharomyces cerevisiae* SAPKs Hog1 and
800 Mpk1 is mediated by glycerol accumulation. *Fungal Biol* **124**: 361-367
801 Lee J, Reiter W, Dohnal I, Gregori C, Beese-Sims S, Kuchler K, Ammerer G, & Levin DE (2013)
802 MAPK Hog1 closes the *S. cerevisiae* glycerol channel Fps1 by phosphorylating and displacing its
803 positive regulators. *Genes Dev* **27**: 2590-2601
804 Lesage G & Bussey H (2006) Cell wall assembly in *Saccharomyces cerevisiae*. *Microbiol Mol Biol*
805 *Rev* **70**: 317-343
806 Leskoske KL, Roelants FM, Martinez Marshall MN, Hill JM, & Thorner J (2017) The Stress-Sensing

807 TORC2 Complex Activates Yeast AGC-Family Protein Kinase Ypk1 at Multiple Novel Sites.
808 *Genetics* **207**: 179-195
809 Levin DE (2011) Regulation of cell wall biogenesis in *Saccharomyces cerevisiae*: the cell wall
810 integrity signaling pathway. *Genetics* **189**: 1145-1175
811 Levin DE (2005) Cell wall integrity signaling in *Saccharomyces cerevisiae*. *Microbiol Mol Biol Rev*
812 **69**: 262-291
813 Levin DE & Bartlett-Heubusch E (1992) Mutants in the *S. cerevisiae PKC1* gene display a cell
814 cycle-specific osmotic stability defect. *J Cell Biol* **116**: 1221-1229
815 Lommel M, Bagnat M, & Strahl S (2004) Aberrant processing of the WSC family and Mid2p cell
816 surface sensors results in cell death of *Saccharomyces cerevisiae* O-mannosylation mutants. *Mol*
817 *Cell Biol* **24**: 46-57
818 Luyten K, Albertyn J, Skibbe WF, Prior BA, Ramos J, Thevelein JM, & Hohmann S (1995) Fps1, a
819 yeast member of the MIP family of channel proteins, is a facilitator for glycerol uptake and efflux
820 and is inactive under osmotic stress. *EMBO J* **14**: 1360-1371
821 Ma H, Snook LA, Kaminskyj SGW, & Dahms TES (2005) Surface ultrastructure and elasticity in
822 growing tips and mature regions of Aspergillus hyphae describe wall maturation. *Microbiology*
823 *(Reading)* **151**: 3679-3688
824 Madden K & Snyder M (1998) Cell polarity and morphogenesis in budding yeast. *Annu Rev Microbiol*
825 **52**: 687-744
826 Maeno A & Akasaka K (2015) High-pressure fluorescence spectroscopy. *Subcell Biochem* **72**: 687-705
827 Marietou A, Nguyen AT, Allen EE, & Bartlett DH (2015) Adaptive laboratory evolution of Escherichia
828 coli K-12 MG1655 for growth at high hydrostatic pressure. *Front Microbiol* **5**: 749
829 Martin H, Rodriguez-Pachon JM, Ruiz C, Nombela C, & Molina M (2000) Regulatory mechanisms
830 for modulation of signaling through the cell integrity Slt2-mediated pathway in *Saccharomyces*
831 *cerevisiae*. *J Biol Chem* **275**: 1511-1519
832 Matsuki H, Goto M, Tada K, & Tamai N (2013) Thermotropic and barotropic phase behavior of
833 phosphatidylcholine bilayers. *Int J Mol Sci* **14**: 2282-2302
834 Merchan S, Bernal D, Serrano R, & Yenush L (2004) Response of the *Saccharomyces cerevisiae* Mpk1
835 mitogen-activated protein kinase pathway to increases in internal turgor pressure caused by loss
836 of Ppz protein phosphatases. *Eukaryot Cell* **3**: 100-107

837 Minc N, Boudaoud A, & Chang F (2014) Mechanical Forces of Fission Yeast Growth. *Curr Biol* **24**:
838 1436
839 Mishra R, Minc N, & Peter M (2022) Cells under pressure: how yeast cells respond to mechanical
840 forces. *Trends Microbiol* **30**: 495-510
841 Mollapour M, Shepherd A, & Piper PW (2009) Presence of the Fps1p aquaglyceroporin channel is
842 essential for Hog1p activation, but suppresses Slt2(Mpk1)p activation, with acetic acid stress of
843 yeast. *Microbiology (Reading)* **155**: 3304-3311
844 Mota MJ, Lopes RP, Delgadillo I, & Saraiva JA (2013) Microorganisms under high
845 pressure--adaptation, growth and biotechnological potential. *Biotechnol Adv* **31**: 1426-1434
846 Muir A, Roelants FM, Timmons G, Leskoske KL, & Thorner J (2015) Down-regulation of
847 TORC2-Ypk1 signaling promotes MAPK-independent survival under hyperosmotic stress. *Elife*
848 **4**: 10.7554/eLife.09336
849 Natenstedt J, Kok AC, Dankelman J, & Tuijthof GJ (2015) What quantitative mechanical loading
850 stimulates in vitro cultivation best? *J Exp Orthop* **2**: 15-015-0029-x. Epub 2015 Jun 19
851 Neeli-Venkata R, Diaz CM, Celador R, Sanchez Y, & Minc N (2021) Detection of surface forces by
852 the cell-wall mechanosensor Wsc1 in yeast. *Dev Cell* **56**: 2856-2870.e7
853 Orlean P (2012) Architecture and biosynthesis of the *Saccharomyces cerevisiae* cell wall. *Genetics*
854 **192**: 775-818
855 Pattappa G, Zellner J, Johnstone B, Docheva D, & Angele P (2019) Cells under pressure - the
856 relationship between hydrostatic pressure and mesenchymal stem cell chondrogenesis. *Eur Cell*
857 *Mater* **37**: 360-381
858 Perrier-Cornet JM, Marechal PA, & Gervais P (1995) A new design intended to relate high pressure
859 treatment to yeast cell mass transfer. *J Biotechnol* **41**: 49-58
860 Peterson J, Zheng Y, Bender L, Myers A, Cerione R, & Bender A (1994) Interactions between the bud
861 emergence proteins Bem1p and Bem2p and Rho-type GTPases in yeast. *J Cell Biol* **127**:
862 1395-1406
863 Philip B & Levin DE (2001) Wsc1 and Mid2 are cell surface sensors for cell wall integrity signaling
864 that act through Rom2, a guanine nucleotide exchange factor for Rho1. *Mol Cell Biol* **21**: 271-280
865 Piao HL, Machado IM, & Payne GS (2007) NPFXD-mediated endocytosis is required for polarity and
866 function of a yeast cell wall stress sensor. *Mol Biol Cell* **18**: 57-65

867 Pruyne D & Bretscher A (2000) Polarization of cell growth in yeast. I. Establishment and maintenance
868 of polarity states. *J Cell Sci* **113 (Pt 3)**: 365-375
869 Ram AF, Wolters A, Ten Hoopen R, & Klis FM (1994) A new approach for isolating cell wall mutants
870 in *Saccharomyces cerevisiae* by screening for hypersensitivity to calcofluor white. *Yeast* **10**:
871 1019-1030
872 Ranade SS, Syeda R, & Patapoutian A (2015) Mechanically Activated Ion Channels. *Neuron* **87**:
873 1162-1179
874 Riggi M, Niewola-Staszkowska K, Chiaruttini N, Colom A, Kusmider B, Mercier V, Soleimanpour S,
875 Stahl M, Matile S, Roux A, & Loewith R (2018) Decrease in plasma membrane tension triggers
876 PtdIns(4,5)P2 phase separation to inactivate TORC2. *Nat Cell Biol* **20**: 1043-1051
877 Rispal D, Eltschinger S, Stahl M, Vaga S, Bodenmiller B, Abraham Y, Filipuzzi I, Movva NR,
878 Aebersold R, Helliwell SB, & Loewith R (2015) Target of rapamycin complex 2 regulates actin
879 polarization and endocytosis via multiple pathways. *J Biol Chem* **290**: 14963-14978
880 Rodicio R & Heinisch JJ (2010) Together we are strong--cell wall integrity sensors in yeasts. *Yeast* **27**:
881 531-540
882 Roelants FM, Baltz AG, Trott AE, Fereres S, & Thorner J (2010) A protein kinase network regulates
883 the function of aminophospholipid flippases. *Proc Natl Acad Sci U S A* **107**: 34-39
884 Roelants FM, Breslow DK, Muir A, Weissman JS, & Thorner J (2011) Protein kinase Ypk1
885 phosphorylates regulatory proteins Orm1 and Orm2 to control sphingolipid homeostasis in
886 *Saccharomyces cerevisiae*. *Proc Natl Acad Sci U S A* **108**: 19222-19227
887 Roelants FM, Torrance PD, Bezman N, & Thorner J (2002) Pkh1 and Pkh2 differentially
888 phosphorylate and activate Ypk1 and Ykr2 and define protein kinase modules required for
889 maintenance of cell wall integrity. *Mol Biol Cell* **13**: 3005-3028
890 Roelants FM, Torrance PD, & Thorner J (2004) Differential roles of PDK1- and
891 PDK2-phosphorylation sites in the yeast AGC kinases Ypk1, Pkc1 and Sch9. *Microbiology*
892 *(Reading)* **150**: 3289-3304
893 Sabir F, Loureiro-Dias MC, Soveral G, & Prista C (2017) Functional relevance of water and glycerol
894 channels in *Saccharomyces cerevisiae*. *FEMS Microbiol Lett* **364**: 10.1093/femsle/fnx080
895 Sakata KT, Hashii K, Yoshizawa K, Tahara YO, Yae K, Tsuda R, Tanaka N, Maeda T, Miyata M, &
896 Tabuchi M (2022) Coordinated regulation of TORC2 signaling by MCC/eisosome-associated

897 proteins, Pil1 and tetraspan membrane proteins during the stress response. *Mol Microbiol* **117**:
898 1227-1244
899 Schaber J, Adrover MA, Eriksson E, Pelet S, Petelenz-Kurdziel E, Klein D, Posas F, Goksor M, Peter
900 M, Hohmann S, & Klipp E (2010) Biophysical properties of *Saccharomyces cerevisiae* and their
901 relationship with HOG pathway activation. *Eur Biophys J* **39**: 1547-1556
902 Schmidt A, Bickle M, Beck T, & Hall MN (1997) The yeast phosphatidylinositol kinase homolog
903 TOR2 activates RHO1 and RHO2 via the exchange factor ROM2. *Cell* **88**: 531-542
904 Schmidt A, Schmelzle T, & Hall MN (2002) The RHO1-GAPs SAC7, BEM2 and BAG7 control
905 distinct RHO1 functions in *Saccharomyces cerevisiae*. *Mol Microbiol* **45**: 1433-1441
906 Schoppner P, Lutz AP, Lutterbach BJ, Bruckner S, Essen LO, & Mosch HU (2022) Structure of the
907 Yeast Cell Wall Integrity Sensor Wsc1 Reveals an Essential Role of Surface-Exposed Aromatic
908 Clusters. *J Fungi (Basel)* **8**: 10.3390/jof8040379
909 Sikorski RS & Hieter P (1989) A system of shuttle vectors and yeast host strains designed for efficient
910 manipulation of DNA in *Saccharomyces cerevisiae*. *Genetics* **122**: 19-27
911 Siliciano PG & Tatchell K (1984) Transcription and regulatory signals at the mating type locus in
912 yeast. *Cell* **37**: 969-978
913 Silva JL, Cordeiro Y, & Foguel D (2006) Protein folding and aggregation: two sides of the same coin
914 in the condensation of proteins revealed by pressure studies. *Biochim Biophys Acta* **1764**:
915 443-451
916 Straede A & Heinisch JJ (2007) Functional analyses of the extra- and intracellular domains of the
917 yeast cell wall integrity sensors Mid2 and Wsc1. *FEBS Lett* **581**: 4495-4500
918 Suzuki A, Mochizuki T, Uemura S, Hiraki T, & Abe F (2013) Pressure-induced endocytic degradation
919 of the *Saccharomyces cerevisiae* low-affinity tryptophan permease Tat1 is mediated by Rsp5
920 ubiquitin ligase and functionally redundant PPxY motif proteins. *Eukaryot Cell* **12**: 990-997
921 Tabuchi M, Audhya A, Parsons AB, Boone C, & Emr SD (2006) The phosphatidylinositol
922 4,5-biphosphate and TORC2 binding proteins Slm1 and Slm2 function in sphingolipid regulation.
923 *Mol Cell Biol* **26**: 5861-5875
924 Tamas MJ, Karlgren S, Bill RM, Hedfalk K, Allegri L, Ferreira M, Thevelein JM, Rydstrom J, Mullins
925 JG, & Hohmann S (2003) A short regulatory domain restricts glycerol transport through yeast
926 Fps1p. *J Biol Chem* **278**: 6337-6345

927 Tamas MJ, Luyten K, Sutherland FC, Hernandez A, Albertyn J, Valadi H, Li H, Prior BA, Kilian SG,
928 Ramos J, Gustafsson L, Thevelein JM, & Hohmann S (1999) Fps1p controls the accumulation
929 and release of the compatible solute glycerol in yeast osmoregulation. *Mol Microbiol* **31**:
930 1087-1104
931 Uemura S, Mochizuki T, Amemiya K, Kurosaka G, Yazawa M, Nakamoto K, Ishikawa Y, Izawa S, &
932 Abe F (2020) Amino acid homeostatic control by TORC1 in *Saccharomyces cerevisiae* under
933 high hydrostatic pressure. *J Cell Sci* **133**: 10.1242/jcs.245555
934 Usami Y, Uemura S, Mochizuki T, Morita A, Shishido F, Inokuchi J, & Abe F (2014) Functional
935 mapping and implications of substrate specificity of the yeast high-affinity leucine permease
936 Bap2. *Biochim Biophys Acta* **1838**: 1719-1729
937 Vay HA, Philip B, & Levin DE (2004) Mutational analysis of the cytoplasmic domain of the Wsc1 cell
938 wall stress sensor. *Microbiology (Reading)* **150**: 3281-3288
939 Wilk S, Wittland J, Thywissen A, Schmitz HP, & Heinisch JJ (2010) A block of endocytosis of the
940 yeast cell wall integrity sensors Wsc1 and Wsc2 results in reduced fitness in vivo. *Mol Genet*
941 *Genomics* **284**: 217-229
942 Winter R (2019) Interrogating the structural dynamics and energetics of biomolecular systems with
943 pressure Modulation. *Annu Rev Biophys* **48**: 441-463
944 Winter R (2002) Synchrotron X-ray and neutron small-angle scattering of lyotropic lipid mesophases,
945 model biomembranes and proteins in solution at high pressure. *Biochim Biophys Acta* **1595**:
946 160-184
947 Winzeler EA, Shoemaker DD, Astromoff A, Liang H, Anderson K, Andre B, Bangham R, Benito R,
948 Boeke JD, Bussey H, Chu AM, Connelly C, Davis K, Dietrich F, Dow SW, El Bakkoury M,
949 Foury F, Friend SH, Gentalen E, Giaever G et al. (1999) Functional characterization of the *S.*
950 *cerevisiae* genome by gene deletion and parallel analysis. *Science* **285**: 901-906
951 Yamaguchi M, Taguchi M, Uematsu K, Takahashi-Nakaguchi A, Sato-Okamoto M, & Chibana H
952 (2021a) Sandwich freezing device for rapid freezing of viruses, bacteria, yeast, cultured cells and
953 animal and human tissues in electron microscopy. *Microscopy (Oxf)* **70**: 215-223
954 Yamaguchi M, Takahashi-Nakaguchi A, Uematsu K, Taguchi M, Sato-Okamoto M, & Chibana H
955 (2021b) Rapid freezing using sandwich freezing device for good ultrastructural preservation of
956 biological specimens in electron microscopy. *J Vis Exp* **(173). doi**: 10.3791/62431

957 Yoshida S, Bartolini S, & Pellman D (2009) Mechanisms for concentrating Rho1 during cytokinesis.
958 *Genes Dev* **23**: 810-823
959 Yoshino D, Funamoto K, Sato K, Kenry, Sato M, & Lim CT (2020) Hydrostatic pressure promotes
960 endothelial tube formation through aquaporin 1 and Ras-ERK signaling. *Commun Biol* **3**:
961 152-020-0881-9
962

Table 1. Strains used in this study

Strains	Genotype	Source or reference
BY4742	*MATα his3*Δ1 *leu2Δ*0 *lys2*Δ0 *ura3*Δ0	(Brachmann et al., 1998)
16672	*wsc1*Δ::*kanMX4* in BY4742	(Winzeler et al., 1999)
11161	*wsc2*Δ::*kanMX4* in BY4742	(Winzeler et al., 1999)
16255	*wsc3*Δ::*kanMX4* in BY4742	(Winzeler et al., 1999)
15241	*mid2*Δ::*kanMX4* in BY4742	(Winzeler et al., 1999)
14653	*mtl1*Δ::*kanMX4* in BY4742	(Winzeler et al., 1999)
14700	*rom1*Δ::*kanMX4* in BY4742	(Winzeler et al., 1999)
15280	*rom2*Δ::*kanMX4* in BY4742	(Winzeler et al., 1999)
16152	*bem2*Δ::*kanMX4* in BY4742	(Winzeler et al., 1999)
14225	*sac7*Δ::*kanMX4* in BY4742	(Winzeler et al., 1999)
13937	*lrg1*Δ::*kanMX4* in BY4742	(Winzeler et al., 1999)
12390	*bag7*Δ::*kanMX4* in BY4742	(Winzeler et al., 1999)
DL100	*MAT*a *his4 leu2-3,112 trp1-1 ura3-52 can1*	(Siliciano & Tatchell, 1984)
DL376	*pkc1*Δ::*Leu2* in DL100	(Levin & Bartlett-Heubusch, 1992)
11328	*bck1*Δ::*kanMX4* in BY4742	(Winzeler et al., 1999)
12487	*mkk1*Δ::*kanMX4* in BY4742	(Winzeler et al., 1999)
12112	*mkk2*Δ::*kanMX4* in BY4742	(Winzeler et al., 1999)
10993	*slt2*Δ::*kanMX4* in BY4742	(Winzeler et al., 1999)
TMY1482	*SWI4-GFP*::*HIS3* in BY4742	This study
12739	*rlm1*Δ::*kanMX4* in BY4742	(Winzeler et al., 1999)
16109	*swi4*Δ::*kanMX4* in BY4742	(Winzeler et al., 1999)
14131	*swi6*Δ::*kanMX4* in BY4742	(Winzeler et al., 1999)
AFY7	*PIL1*-mCherry::*URA3* in BY4742	(Ishii et al., 2022)
MSY1	*NCE102*-mCherry::*URA3* in BY4742	This study
MSY17	*SUR7*-mCherry::*URA3* in BY4742	This study
11531	*fps1*Δ::*kanMX4* in BY4742	(Winzeler et al., 1999)
11446	*gpp1*Δ::*kanMX4* in BY4742	(Winzeler et al., 1999)
10199	*gpp2*Δ::*kanMX4* in BY4742	(Winzeler et al., 1999)
13718	*gpd1*Δ::*kanMX4* in BY4742	(Winzeler et al., 1999)
11751	*gpd2*Δ::*kanMX4* in BY4742	(Winzeler et al., 1999)
TTY146	*fps1*Δ::*HphMX6 gpp1*::*kanMX4* in BY4742	This study
TTY147	*fps1*Δ*::HphMX6 gpd1*::*kanMX4* in BY4742	This study
TTY108	*SLM1-GFP*::*HIS3 LSP1-mCherry*::*URA3* in BY4742	This study
TTY113	*SLM1-GFP::HIS3 AVO3-3×mCherry*::*URA3* in BY4742	This study
14976	*ypk1*Δ::*kanMX4* in BY4742	(Winzeler et al., 1999)

Table 2. Plasmids used in this study

Plasmid	Description	Source or reference
pUA35	3HA *URA3 CEN*4	Laboratory stock
pTM35	*GFP URA3 CEN*4	Laboratory stock
YEplac181	*LEU2 2 μ*	(Gietz & Sugino, 1988)
YCplac22	*TRP1 CEN4*	(Gietz & Sugino, 1988)
pRS313	*HIS3 CEN6*	(Sikorski & Hieter, 1989)
pTAT1-GFP	*TAT1*-GFP driven by its own promoter in pRS313	This study
pMB1	*WSC1*-3HA driven by its own promoter in pUA35	This study
pMB23	*WSC1*-3HA-Y303A driven by its own promoter in pUA35	This study
pMB74	*WSC1*-3HA-N344A-P345A-F346A driven by its own promoter in pUA35	This study
pSS21	*WSC1*-GFP driven by its own promoter in pTM35	This study
pMB80	*WSC1*-3HA-N344A-P345A-F346A driven by its own promoter in pTM35	This study
SP333	HA-*RHO1* driven by its own promoter *LEU2 CEN*	(Yoshida et al., 2009)
SP335	HA-*RHO1*-F35L driven by its own promoter *LEU2 CEN*	(Yoshida et al., 2009)
SP336	HA-*RHO1*-Q68H driven by its own promoter *LEU2 CEN*	(Yoshida et al., 2009)
pME29	*PKC1* driven by its own promoter in YEplac181	This study
pME30	*PKC1*-R398P driven by its own promoter in YEplac181	This study
pTNK5	*FPS1* driven by its own promoter in pUA35	This study
pTNK8	*FPS1*-T231A driven by its own promoter in pUA35	This study
pTNK9	*FPS1*-S537A driven by its own promoter in pUA35	This study
pTNK10	*FPS1*-S570A driven by its own promoter in pUA35	This study
pTNK22	*FPS1*-S181A-S185A driven by its own promoter in pUA35	This study
pTNK23	*FPS1*-S181A-S185A-S570A driven by its own promoter in pUA35	This study
pTNK15	*FPS1*-Δ11 driven by its own promoter in pUA35	This study
pSS10	*FPS1*-3HA driven by its own promoter in pUA35	This study
pSS26	*FPS1*-3HA-S537A driven by its own promoter in pUA35	This study
pSS12	*FPS1*-3HA-S570A driven by its own promoter in pUA35	This study
pSS16	*FPS1*-3HA-S181A-S185A driven by its own promoter in pUA35	This study
pSS14	*FPS1*-3HA-S181A-S185A-S570A driven by its own promoter in pUA35	This study
pSS6	*YPK1* driven by its own promoter in pUA35	This study
pTNK11	*YPK1*-S51A-S71A driven by its own promoter in pUA35	This study
pTNK7	*YPK1*-T504A driven by its own promoter in pUA35	This study
pTNK14	*YPK1*-S644A-T662A driven by its own promoter in pUA35	This study
pTM102	pBSK (+) -*SFK1*-3×mCherry	(Kishimoto et al., 2021)
pJT6	GFP *HIS3*	(Kawada et al., 2015)
pJT601	mCherry *URA3*	(Kawada et al., 2015)

963 **Figure legends**

964 Fig. 1. Schematic representation of the CWI pathway in *Saccharomyces cerevisiae*. Five cell wall
965 sensor proteins are depicted. Upon cell wall stress, Wsc1 first clusters at the cell surface. Binding of
966 the GDP/GTP exchanging factor, Rom2, to the cytoplasmic tail of Wsc1 activates the small GTPase,
967 Rho1. Rho1-GTP activates the protein kinase C, Pkc1, which activates a conserved mitogen-activated
968 protein kinase (MAPK) cascade. The cascade consists of Bck1 (MAPKKK), Mkk1/Mkkk2
969 (MAPKKs), and Slt2 (MAPK). Phosphorylated Slt2 translocates into the nucleus and promotes cell
970 cycle progression through the SBF complex and transcription of genes encoding cell wall proteins by
971 Rlm1. Slt2 also phosphorylates aquaglyceroporin, Fps1, and promotes Fps1 opening to expel glycerol.
972 When cells are stressed, tension is applied to the plasma membrane, causing the loss of the eisosome,
973 a plasma membrane invaginating structure. Slm1/Slm2 localized in the eisosome migrate to TORC2.
974 Consequently, TORC2 is activated and phosphorylates Ypk1. Phosphorylated Ypk1 also
975 phosphorylates Fps1, positively regulating glycerol efflux. The phosphorylation sites, kinases, and
976 functional motifs in major proteins used in this study are outlined below. CRD (8C), cysteine-rich
977 domain (C27, C49, C53, C69, C71, C86, C90, and C98); STR, serine/threonine-rich domain (111–265
978 amino acid residues); NPF motif, N344-P345-F346.

979

980 Fig. 2. Wsc1 is required for growth under high pressure. (A) Wild-type and mutant cells were cultured
981 in SC medium at 0.1 MPa or 25 MPa for 48 h with an initial OD_{600} = 0.01. Unless otherwise specified,
982 the high-pressure growth test was carried under this condition throughout the experiments. (B)
983 Wild-type cells were cultured in SC medium containing various concentrations of caspofungin at 0.1
984 MPa or 25 MPa. The IC_{50} values were derived from the plots. (C) Cells with mutations in the
985 extracellular domain of Wsc1 were cultured in SC medium at 0.1 MPa or 25 MPa. (D). Wild-type cells
986 expressing Wsc1-GFP or $Wsc1^{NPF>AAA}$-GFP were cultured at 0.1 MPa or 25 MPa for 3 h and were
987 observed under a confocal laser microscope immediately after depressurization. (E) *wsc1*Δ cells
988 expressing Wsc1 or $Wsc1^{NPF>AAA}$ were cultured at 0.1 MPa or 25 MPa. Data are presented as mean ±
989 standard deviation of three independent experiments.

990

991 Fig. 3. CWI pathway is activated by high pressure. (A) Mutant strains, with various defects in the CWI
992 pathway, were cultured in SC medium at 0.1 MPa or 25 MPa. (B) *rom2*Δ cells expressing Rho1 or

993 Pck1 derivatives were cultured in SC medium at 0.1 MPa or 25 MPa. (C) Mutant strains, with various
994 defects in the CWI pathway, were cultured in SC medium at 0.1 MPa or 25 MPa. Note that strains
995 DL100 and DL376 harboring YCplac22 (*TRP1, CEN*) were used to examine the *PKC1* deficiency
996 (left). (D) Wild-type cells were cultured in SC medium under various pressure conditions for 3 h. Slt2
997 and phosphorylated Slt2 (P-Slt2) were detected by western blotting using specific antibodies. The
998 relative intensities, P-Slt2/Adh1 and Slt2/Adh1, were quantified in an ImageQuant LAS4000 mini. (E)
999 Wild-type cells expressing Swi4-GFP were incubated with 15 μg/mL nocodazole for 2 h at 0.1 MPa.
1000 The cells were then cultured for another 5 h at 0.1 MPa or 25 MPa and were observed after
1001 depressurization. The percentages of cells with Swi4-GFP in the nucleus in more than 300 cells are
1002 shown. (F) Mutant strains were cultured in SC medium at 0.1 MPa or 25 MPa. Data are presented as
1003 mean ± standard deviation of three independent experiments.
1004
1005 Fig. 4. High pressure causes cell swelling and loss of the eisosome structure. (A) Wild-type cells
1006 co-expressing Tat1-GFP (plasma membrane marker) and Nce102-mCherry (eisosome marker) were
1007 cultured in SC medium at 0.1, 25 or 50 MPa for 3 h and were observed under a confocal laser
1008 microscope after depressurization. Cross-section images are shown. (B) Cells co-expressing Tat1-GFP
1009 and Nce102-mCherry, Pil1-mCherry or Sur7-mCherry were cultured in SC medium at 0.1 MPa or 25
1010 MPa for 1 h or 3 h. Pearson's correlation coefficient (PCC) was obtained for cell surface images from
1011 63 cells in three independent experiments. (C) Changes in cell volume when cultured under high
1012 pressure. Cells were cultured at 0.1, 25 or 50 MPa for 1 h or 3 h in SC medium with or without 1 M
1013 sorbitol. The cell volume was calculated from the cell diameter of more than 300 cells after
1014 depressurization in three independent experiments.
1015
1016 Fig. 5. Glycerol efflux via Aquaglyceroporin Fps1 is required for high-pressure growth. (A) The CFW
1017 sensitivity is enhanced under high pressure. Wild-type cells were cultured in SC medium with or
1018 without CFW at 0.1 MPa or 25 MPa. (B) Wild-type and *fps1*Δ cells were cultured in SC medium with
1019 or without 1 M sorbitol at 0.1 MPa or 25 MPa. (C) Mutants defective in glycerol synthesis were
1020 cultured in SC medium at 0.1 MPa or 25 MPa. (D) Measurement of intracellular and extracellular
1021 glycerol levels after incubating cells at 0.1 MPa or 25 MPa for 24 h with an initial OD_{600} = 0.1.
1022 Glycerol levels were quantified using a Glycerol assay kit. Data are presented as mean ± standard

1023 deviation of three independent experiments.

1024

1025 Fig. 6. Ultrastructure of the cells observed by transmission electron microscopy. Wild-type and *fps1*Δ
1026 cells were cultured at 0.1 MPa or 25 MPa for 24 h, and after depressurization, the samples were
1027 subjected to rapid freezing using the sandwich method. In *fps1*Δ cells, the points of cell wall breakage
1028 are indicated by arrows. Scale bars, 1.0 μm

1029

1030 Fig. 7. Slt2-dependent phosphorylation of Fps1 is required for growth under high pressure. (A) The
1031 Fps1 phosphorylation-site mutants were cultured in SC medium at 0.1 MPa or 25 MPa. (B)
1032 Electrophoretic mobility of Fps1-3HA and its mutant forms was analyzed by western blotting. Cells
1033 were cultured at 0.1 MPa or 25 MPa for 3 h and whole cell extracts were prepared. The arrowhead
1034 indicates a higher-molecular weight band of phospho-Fps1 (P-Fps1). The relative intensities,
1035 P-Fps1/Pma1 at 0.1 MPa and 25 MPa, were quantified in an ImageQuant LAS4000 mini. (C)
1036 Wild-type and *slt2*Δ cells were cultured in SC medium with or without 1 M sorbitol at 0.1 MPa or 25
1037 MPa. (D) *fps1*Δ and *slt2*Δ cells expressing constitutively active Fps1-Δ11 were cultured in SC medium
1038 at 0.1 MPa or 25 MPa. Data are presented as mean ± standard deviation of three independent
1039 experiments. (E) The Ypk1 phosphorylation-site mutants were cultured in SC medium at 0.1 MPa or
1040 25 MPa. (F) The Fps1 phosphorylation-site mutants were cultured in SC medium at 0.1 MPa or 25
1041 MPa.

1042

1043 Fig. 8. Model depicting Wsc1-dependent high-pressure signaling pathway in yeast. When pressure is
1044 applied to the cell, an excessive influx of water into the cell occurs. Perturbation of the cell wall by
1045 high pressure causes further water influx and the cell is at risk of rupture. To prevent this, Wsc1
1046 detects cell wall stretching and activates the CWI pathway. Once the CWI pathway is activated, Slt2
1047 kinase phosphorylates aquaglyceroporin Fps1. Phosphorylated Fps1 promotes its opening, which
1048 allows cells to expel glycerol, adjusting the osmotic pressure balance across the plasma membrane.
1049 TORC2-Ypk1 pathway is independent of the regulation of Fps1 under high pressure.

1050

1051 Fig. S1. TORC2-mediated Ypk1 phosphorylation by high pressure. (A) High pressure causes
1052 dissociation of a fraction of Slm1 from the eisosomes and its migration to TORC2. Wild-type cells

1053 co-expressing Slm1-GFP and Lsp1-mCherry, or those co-expressing Slm1-GFP and Avo3-3×mCherry,
1054 were cultured in SC medium at 0.1 MPa or 25 MPa for 5 h. The cells were observed by confocal laser
1055 microscopy immediately after depressurization. Colocalizations were analyzed in more than 50 cells
1056 from three independent experiments using the cellSens software and represented by the PCC. (B) High
1057 pressure promotes the phosphorylation level of Ypk1. Ypk1 and phosphorylated Ypk1 were detected
1058 from whole cell extracts by western blotting, using antibodies for Ypk1 and phospho-PKC (pan) (zeta
1059 Thr410) (190D10), respectively. The relative intensities, P-Ypk1/Adh1 and Ypk1/Adh1, were
1060 quantified in an ImageQuant LAS4000 mini.
1061
1062

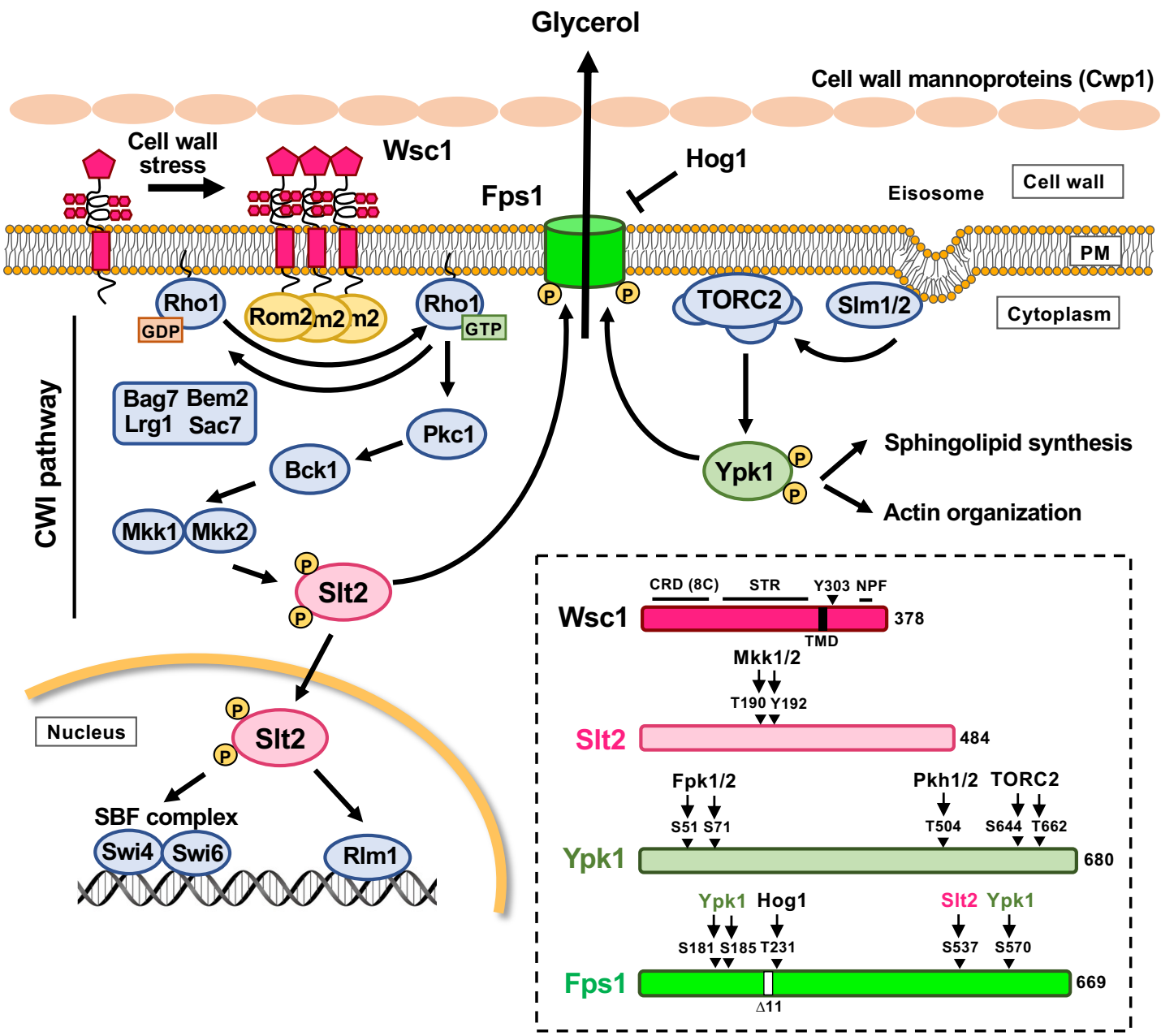

Fig. 1. Mochizuki *et al.*

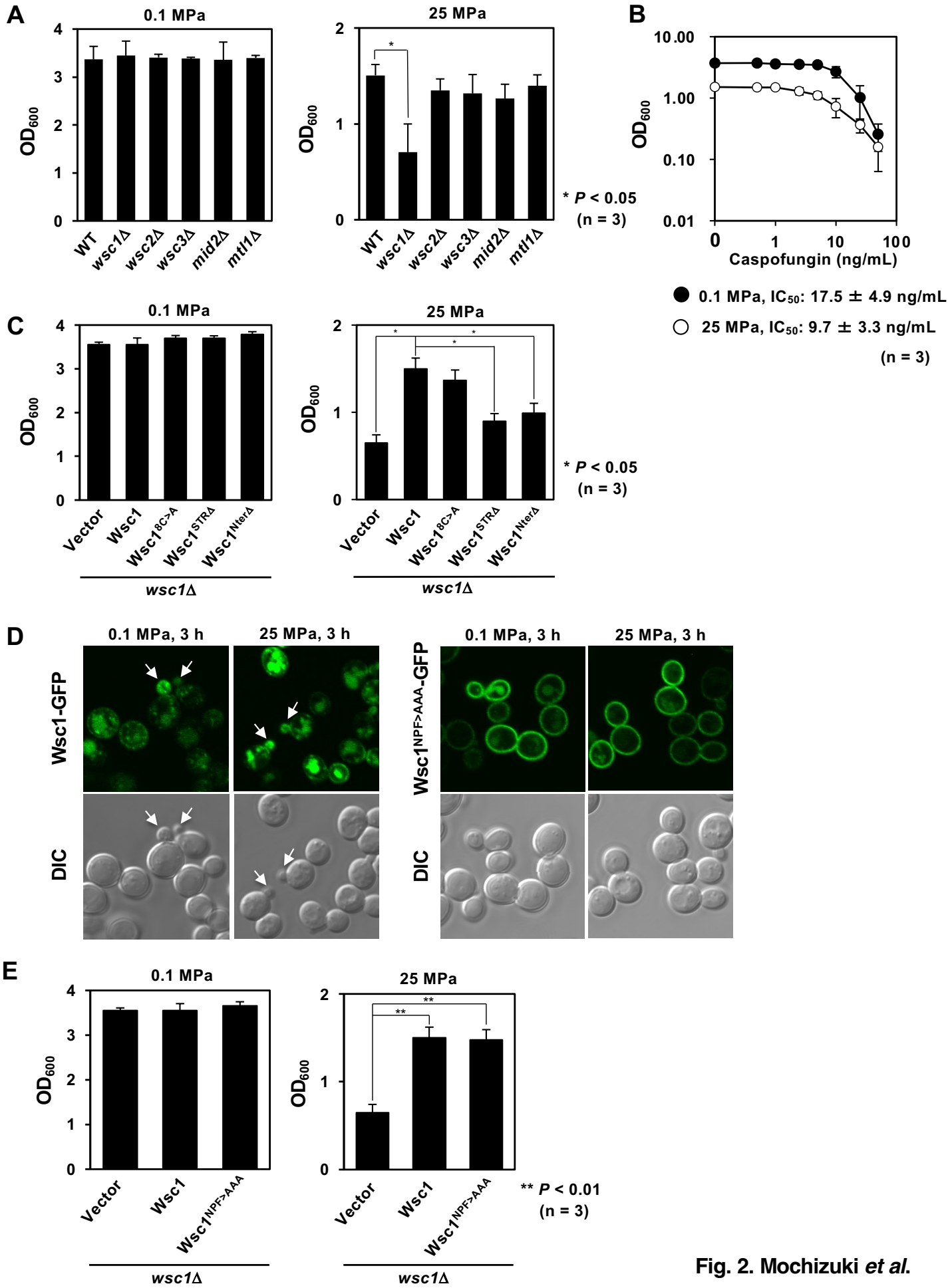

Fig. 2. Mochizuki *et al.*

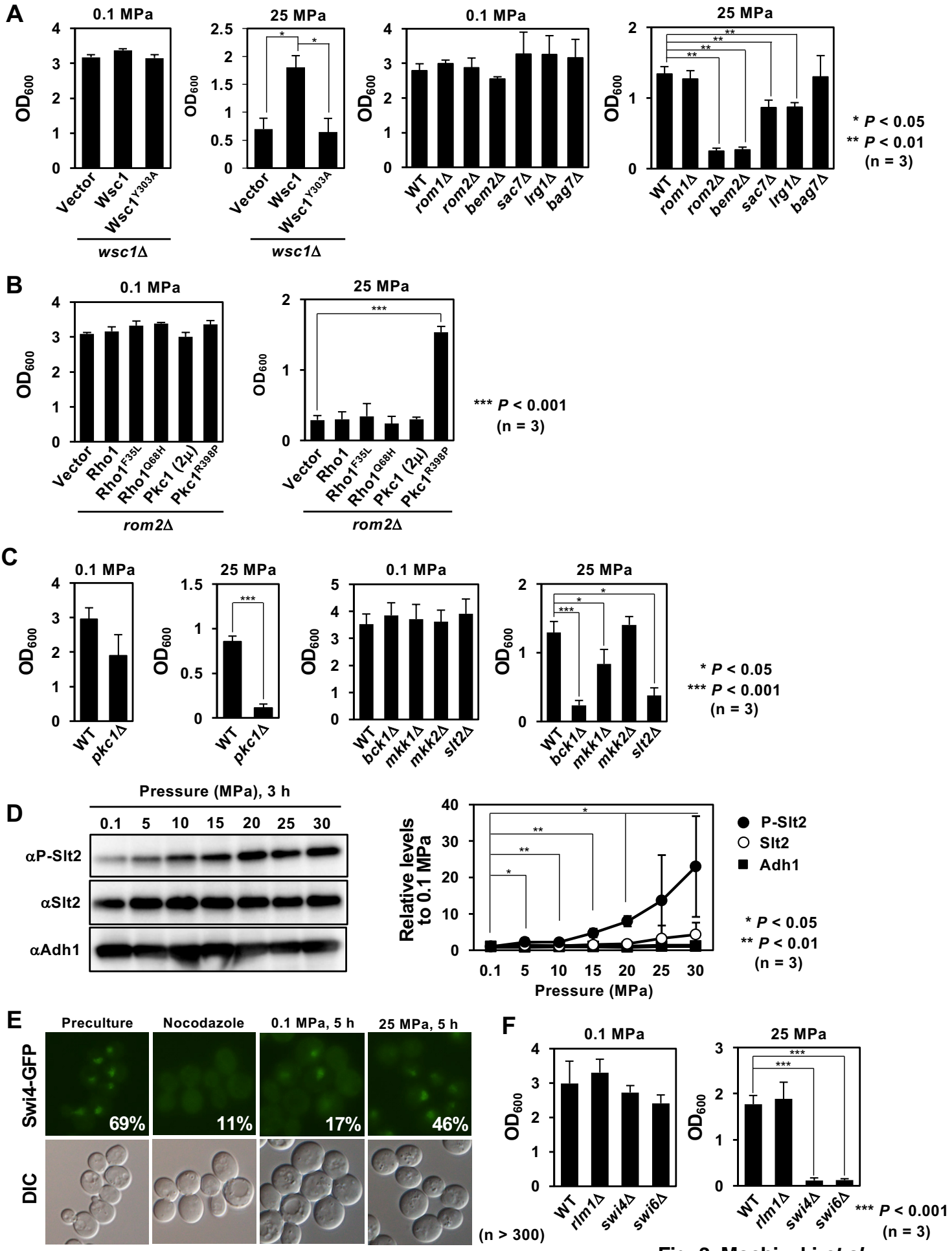

Fig. 3. Mochizuki *et al.*

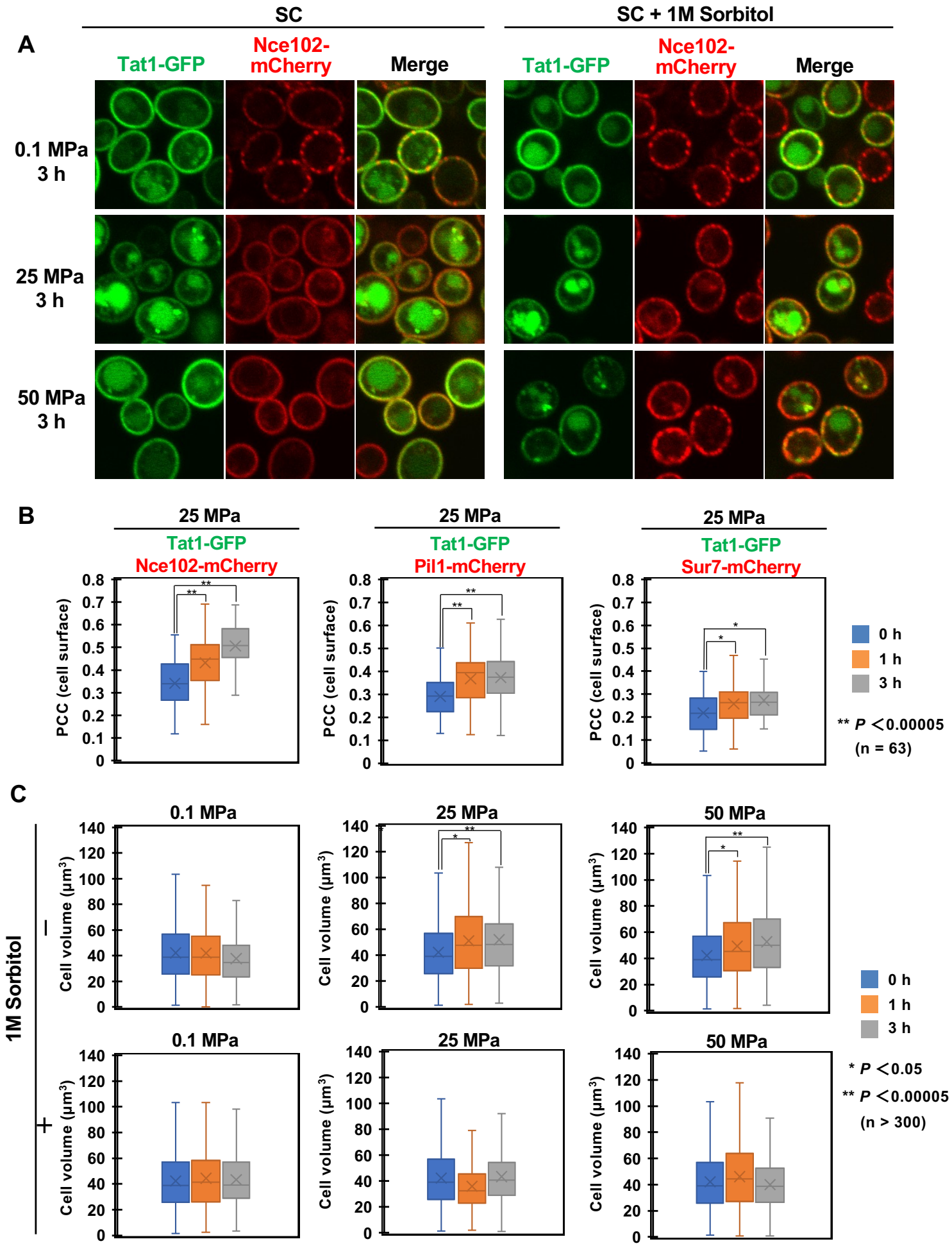

Fig. 4. Mochizuki *et al.*

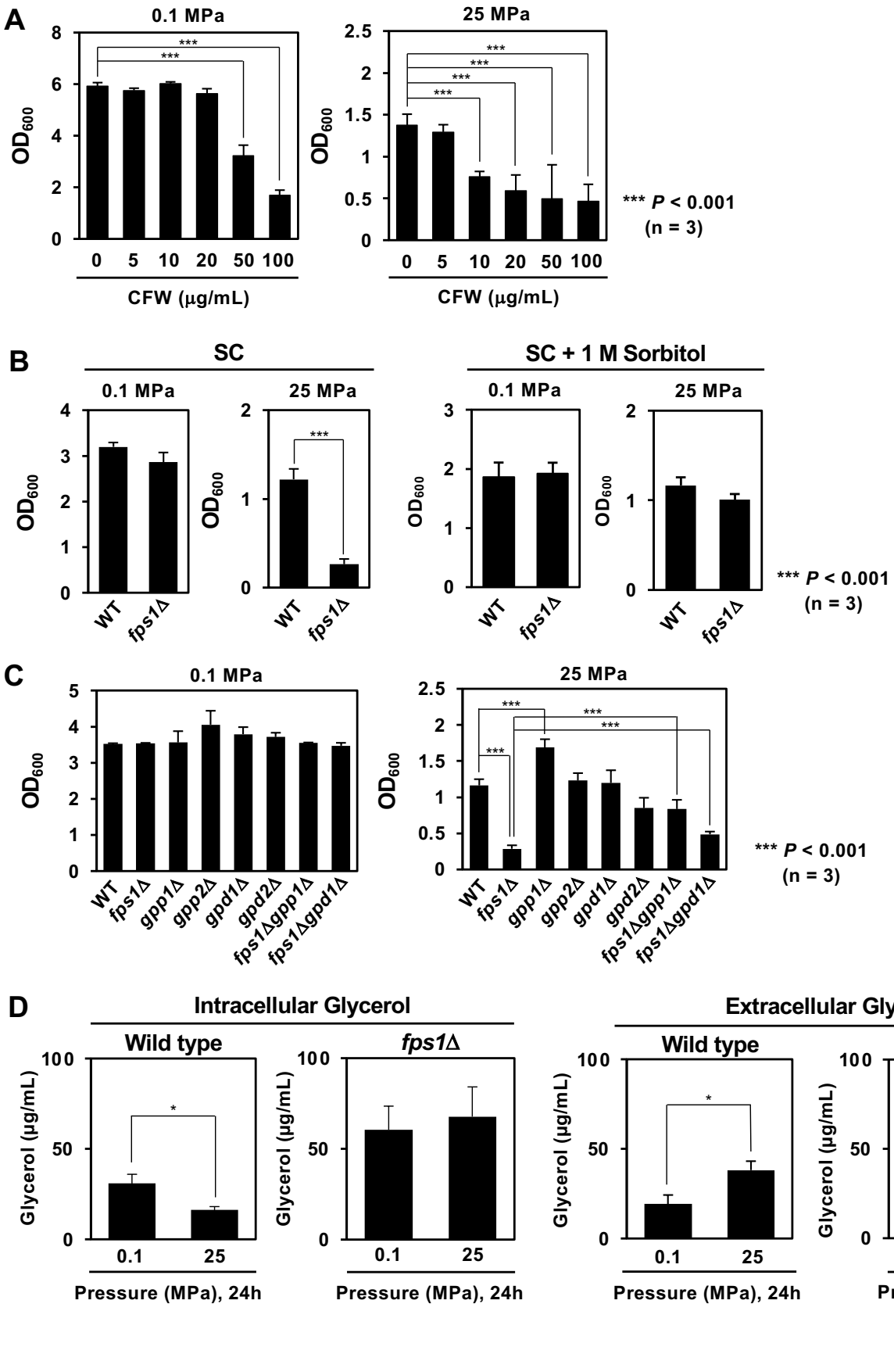

Fig. 5. Mochizuki *et al.*

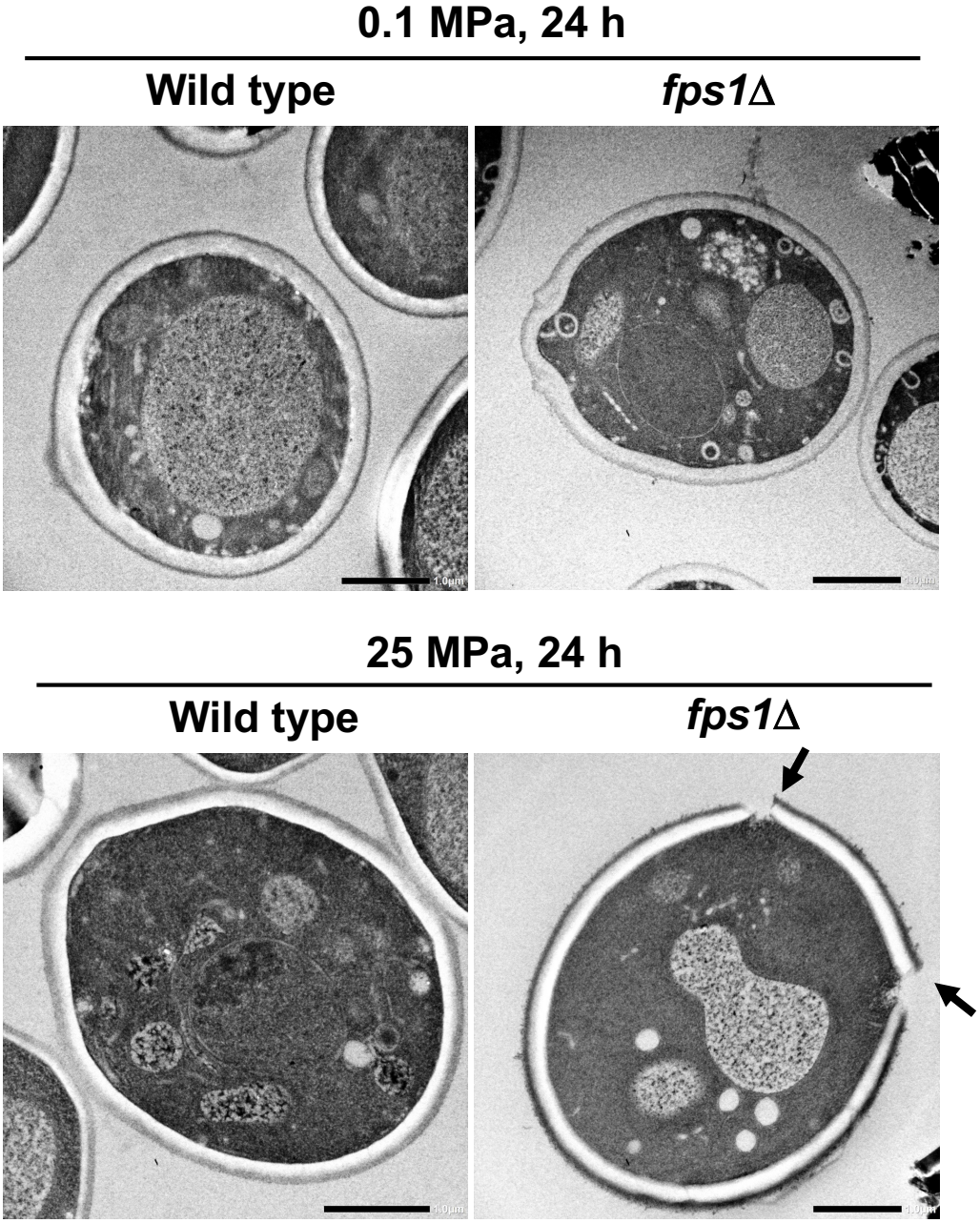

Fig. 6. Mochizuki *et al*.

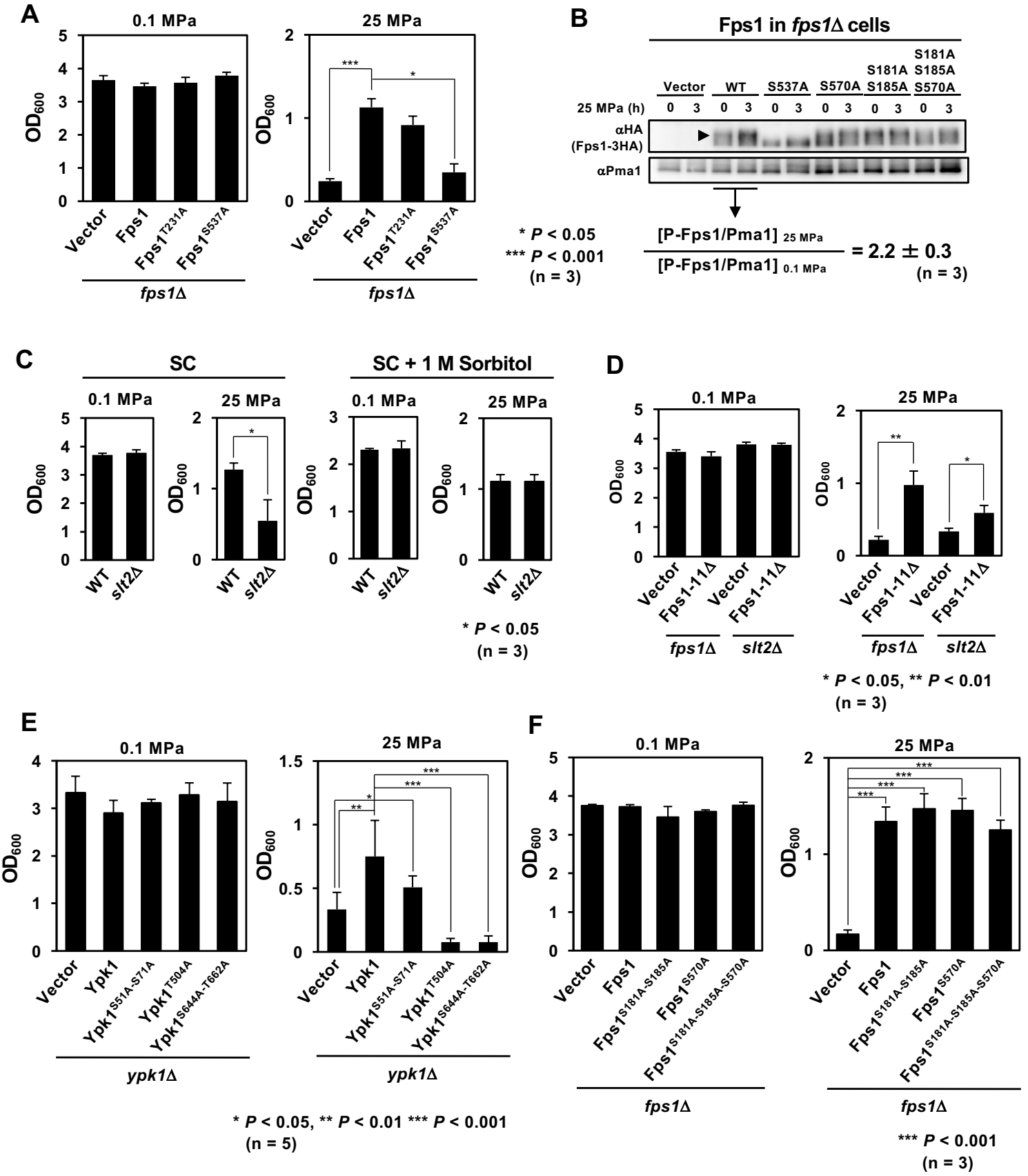

Fig. 7. Mochizuki *et al.*

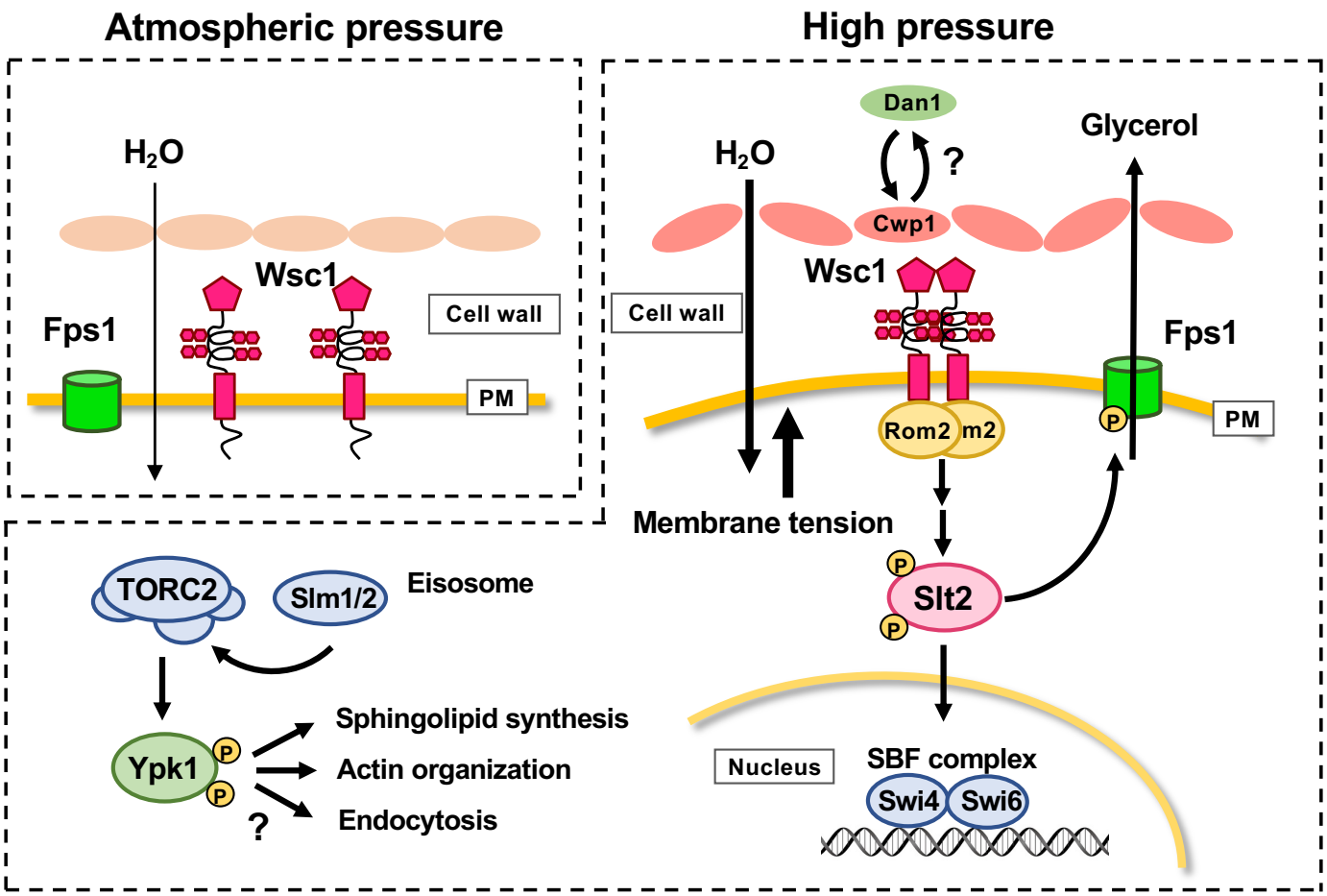

Fig. 8. Mochizuki *et al.*

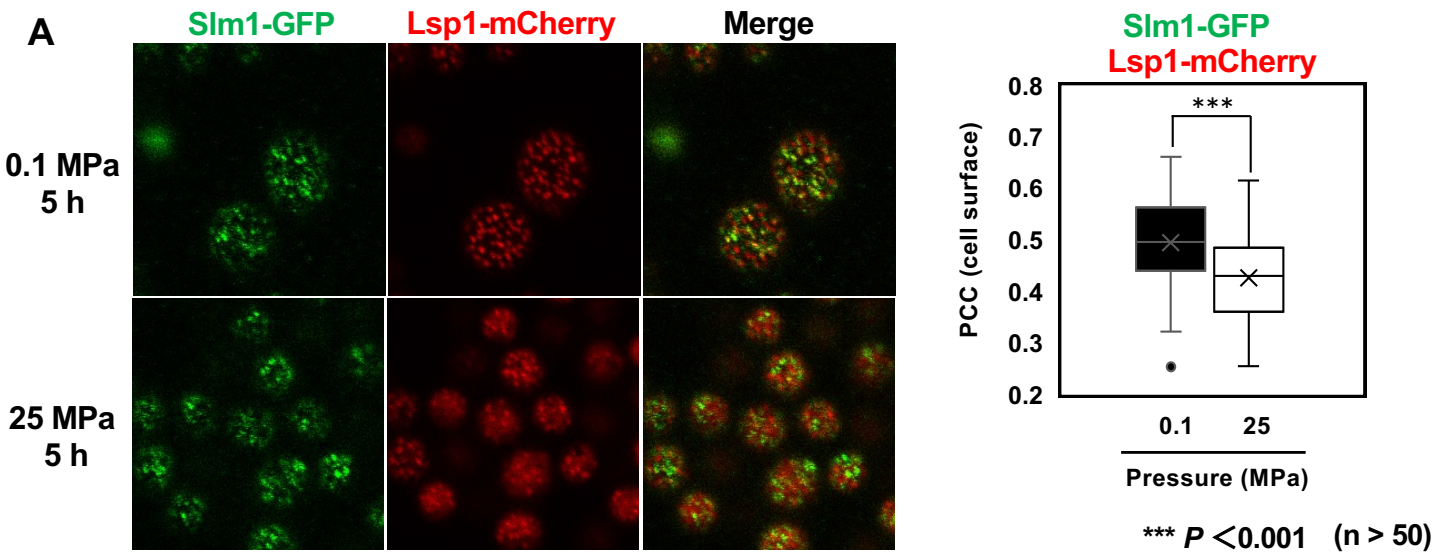

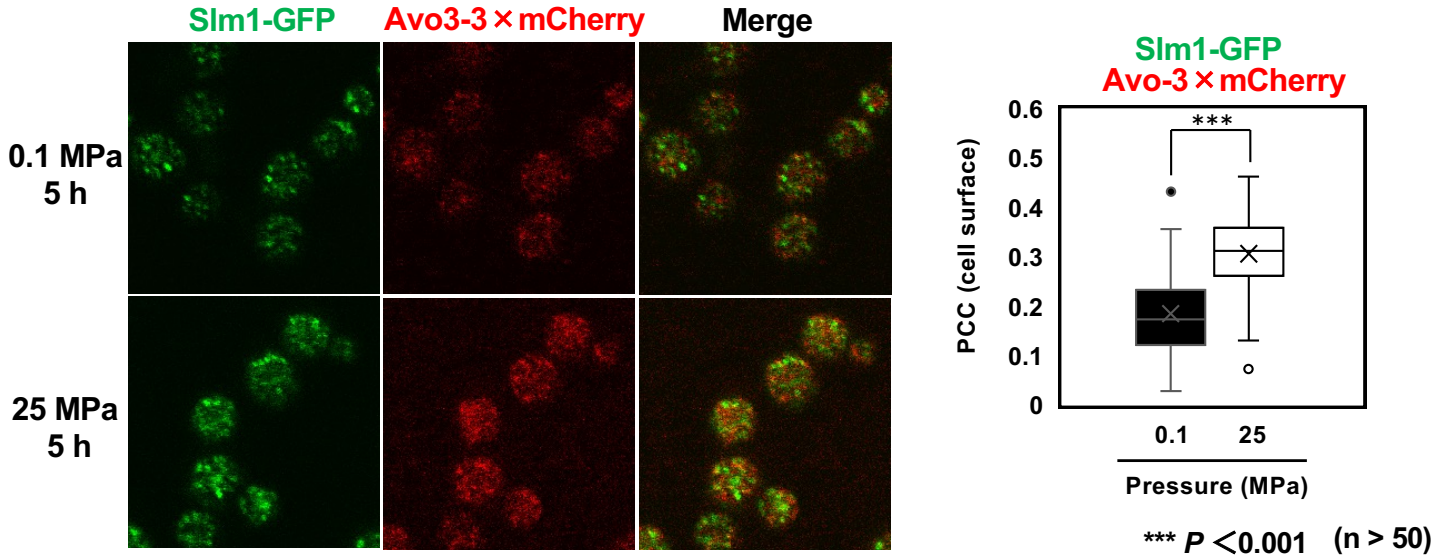

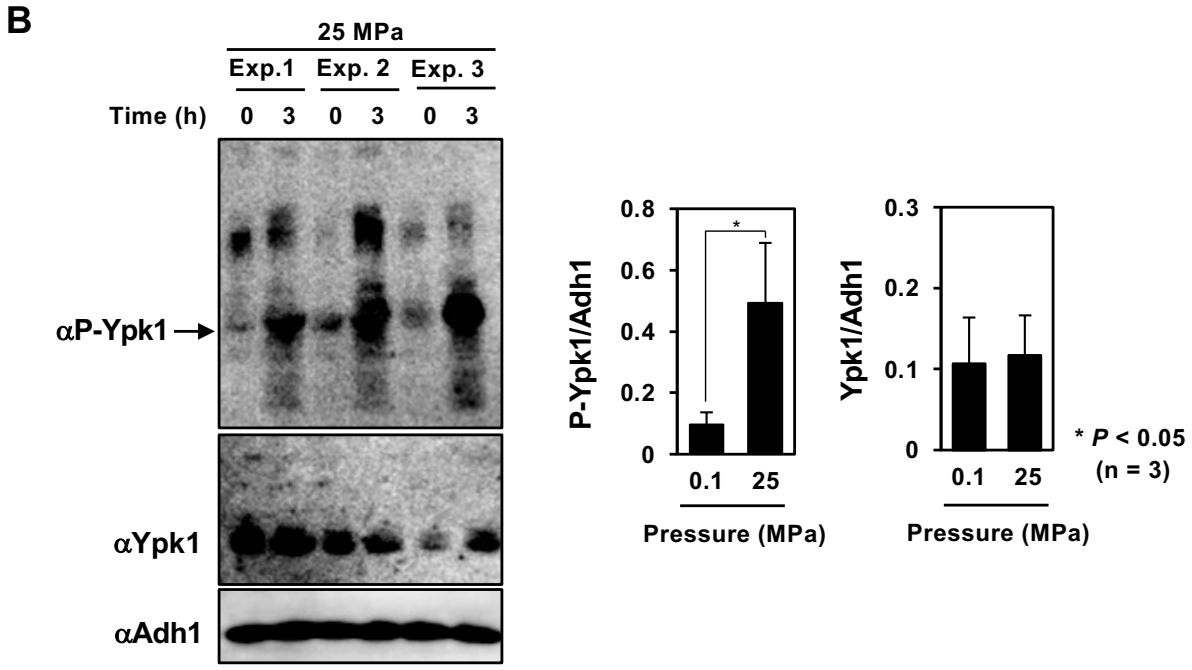

Fig. S1. Mochizuki *et al.*